VALIDATION AND CHARACTERIZATION OF TCF7L1-SALL4 PROTEIN-PROTEIN INTERACTION IN MOUSE EMBRYONIC STEM CELLS

VALIDATION AND CHARACTERIZATION OF TCF7L1-SALL4 PROTEIN-PROTEIN INTERACTION IN MOUSE EMBRYONIC STEM CELLS

BY

CALEB SEO, B.Sc. (Honours)

A Thesis

Submitted to the School of Graduate Studies

In Partial Fulfillment of the Requirements

For the Degree

Master of Science

DESCRIPTIVE NOTE

MASTER OF SCIENCE (2019) McMaster University
(Biochemistry) Hamilton, Ontario

TITLE: Validation and Characterization of TCF7L1-SALL4 Protein-Protein Interaction in Mouse Embryonic Stem Cells

AUTHOR: Caleb Seo, B.Sc. (Honours)

SUPERVISOR: Dr. Bradley Doble

NUMBER OF PAGES: xii, 62

ABSTRACT

Here, we validate novel protein interactors of TCF7L1 (also known as TCF3), a downstream transcription factor in the Wnt/β-catenin signaling pathway, from an initial protein interaction screen that utilized the BioID system in mouse embryonic stem cells. The BioID-TCF7L1 screen identified multiple proteins including several transcription factors and numerous epigenetic regulators. Notably, SALL4, a key embryonic stem cell factor belonging to the SPALT family of transcription factors was validated to interact with TCF7L1 through Proximity Ligation Assay (PLA), and Co-Immunopreciptation (Co-IP). Analysing mRNA transcriptomic signatures of TCF7L1-null mESCs and SALL4 overexpressing mESCs, we observed similarly increased output of the pluripotency-gene, Tbx3, suggesting a transcriptionally opposing function between TCF7L1 and SALL4. Furthermore, we identified that SALL4 also interacted with TCF7, suggesting that SALL4 may interact with all four members of the TCF/LEF transcription factor family to regulate Wnt targets. This work further validates the utility and effectiveness of screening transcription factor interactors through the BioID system and provides important insights into SALL4 mediated Wnt regulation through the TCF/LEFs.

ACKNOWLEDGEMENTS

What a journey it has been. I must say the two years have flew by and the love and support from select people have made my time as a master student a rewarding one.

Most importantly, I would like to thank Dr. Bradley Doble for granting me the opportunity to develop as a competent scientist by providing me with one to one discipleship and the necessary reagents to conduct experiments. Dr. Bradley Doble has always challenged me to think critically and guided me to generate scientifically rationale answers and hypotheses. Thanks to Brad, my curiosity for Wnt signaling is always at its highest point. I can confidently say that I think about research questions and generate hypotheses even when I'm outside the lab doing other activities which I think is a valuable trait in a scientist. Best of luck at the University of Manitoba Brad. Your future graduate students in Manitoba are lucky.

Secondly, among the Doble lab I would like to distinguishingly thank Dr. Steven Moreira. We didn't start off as closest of friends, but over the years I've had the honor of working with you, you've become one of my closest friends and an excellent mentor. My project and how far I've come with it would not have been possible without your prior work on building its foundation and your patience to teach me scientific techniques. Again, congratulations on your receiving your PhD.

I would also like to thank Victor Gordon for helping me interpret scientific data and taking the time to make my transition to the SCC-RI institute a smooth one.

Thanks Smarth for helping me with qPCR and making my graduate student life fun and enjoyable.

I'm also thankful for the excellent high-end facility and equipment provided by the SCC-RI institute which allowed me to perform my experiments with ease and reproducibility.

I would like to lastly thank my family and friends who have unwaveringly supported me throughout this journey both financially and motivationally. Without your comfort and faith in my ability to persevere I would not be where I am today. Thank You.

TABLE OF CONTENTS

LIST OF FIGURES

LIST OF TABLES

LIST OF ABBREVIATIONS

	Abbreviation	Full Form
A	APC	Adenomatous polyposis coli
	ARID1A	AT-rich interactive domain-containing protein 1a
B	bHLH	basic Helix-Loop-Helix
	β-TrCP	Beta-transducin repeats-containing proteins
C	Cas9	CRISPR-associated protein 9
	CK1	Casein kinase 1
	Co-IP	Co-immunoprecipitation
	ChIP	Chromatin immunoprecipitation
	CRISPR	Clustered regularly interspaced short palindromic repeats
	CMV	Cytomegalovirus
D	DPPA3	Developmental pluripotency-associated protein 3
	Dsh	Dishevelled
E	*E. coli*	*Escherichia coli*
	ERK	Extracellular signal-regulated kinase
	ESC	Embryonic stem cell
F	FGF	Fibroblast growth factor
G	GSK3	Glycogen synthase kinase-3
H	hESC	Human embryonic stem cell
	HMG	High Mobility Group
I	ICM	Inner cell mass
	IF	Immunofluorescence
J	JMJD1C	Jumonji domain containing 1c
K	Kbp	Kilobase pair
	kDa	Kilodalton
	KO	Knockout

L	LEF	Lymphoid enhancer factor
	LIC	Ligase-independent cloning
	LRP	Low-density lipoprotein receptor-related protein
M	mESC	Mouse embryonic stem cell
	MNase	Micrococcal nuclease
N	NES	Nuclear export signal
	NLS	Nuclear localization signal
	NPC	Nuclear pore complex
P	PCR	Polymerase chain reaction
Q	QKO	Quadruple knockout
	qPCR	Quantitative polymerase chain reaction
R	RPL13a	Ribosomal protein 13a
S	SALL4	Sal-like 4
	shRNA	Short-hairpin RNA
T	Tbx3	T-box3
	TCF	T-cell Factor
	TLB	TCF/LEF/β-catenin
	TLE	Transducin-like enhancer of split
W	Wnt	Wingless / Integration
	WRE	Wnt-responsive element
	WT	Wild-type

DECLARATION OF ACADEMIC ACHIEVEMENT

The majority of this thesis was completed by Caleb Seo, with the following contributions from members of the Doble lab:

i. Enio Polena generated the TCF/LEF quadruple knockout (QKO) cell line.
ii. Steven Moreira generated the TCF3 KO, TCF3-3xFLAG, TCF1-3xFLAG cell lines.
iii. Smarth Narula generated the TCF/LEF/β-catenin KO (TLB) cell line.

CHAPTER 1: INTRODUCTION

1.1 Embryonic Stem Cells

1.1.1 Derivation

Embryonic stem cells (ESC) are pluripotent stem cells that have the potential to differentiate into all cell types. ESCs were first isolated in 1981 and were successfully cultured after intensive research efforts (Martin, 1981). From the inner cell mass (ICM) of a blastocyst, an early stage pre-implantation embryo, ESCs can be derived and successfully cultured in a defined media comprising hormones, cytokines, and other essential nutrients (Thomson, J. a., Itskovitz-Eldor, 1998). Under such defined conditions, ESCs are able to propagate indefinitely, remaining in an undifferentiated state. They can be induced to differentiate into specific cell types upon altered culturing conditions that activate or supress key cellular signals (Ying, Nichols, Chambers, & Smith, 2003). ESCs can differentiate into primitive ectoderm and further differentiate into the three germ layers consisting of ectoderm, endoderm and mesoderm, and can ultimately give rise to over 220 cell types. (Keller, 1995; Smith, 2001)

1.1.2 Pluripotency and ESC Characterization

Pluripotent cells are distinguishable by several characteristics. A key component of a pluripotent cell is an active core pluripotency transcription factor network consisting of Oct4, Sox2, and Nanog, which are autoregulatory, as individual factors can drive expression of the others by promoter binding (Laurie A. Boyer, 2005). In addition to a faster growth rate, due to an abbreviated G1 phase of the cell cycle, pluripotent cells have a large nucleus which takes up the vast majority of the cell volume (Becker, Ghule, & Stein, 2006; Sathananthan, Pera, & Trounson, 2002).

Currently, there exist both *in vivo* and *in vitro* assays that can be utilized to determine the pluripotent status of stem cells. Assays such as qPCR and Western blotting can be implemented to monitor for key transcripts or proteins that act as markers for different states of the cell. The golden standard tests for pluripotency are chimera formation and tetraploid complementation.

In chimera formation testing, the ESCs being tested are injected into host embryos at the blastocyst stage of development. This results in a chimeric organism that is composed of cells from both the host embryo and the injected ESCs. Chimeras are assessed for the ability of constituent ESCs to mature into functional germline cells such as spermatozoa of chimeric male animals (Mascetti & Pedersen, 2016).

Tetraploid embryos can be produced by employing an electrical current to fuse together 2-cell stage embryos. Resultant tetraploid single-cell embryos continue to divide normally and reach the blastocyst stage; however, they are only able to produce extra-embryonic tissues such as the placenta. In the tetraploid complementation assay, only complementation of tetraploid embryos with pluripotent ESCs can ultimately give rise to an embryo proper containing all three germ layers of endoderm, mesoderm, and ectoderm lineages (Hadjantonakis, MacMaster, & Nagy, 2002; Kwon, Viotti, & Hadjantonakis, 2016).

Another *in vivo* assay for testing pluripotency is the teratoma assay. Teratomas are benign tumours of cellular mixtures comprising the previously mentioned germ layers. In a teratoma assay, ESCs are injected into an immunocompromised or syngeneic mouse and are allowed to grow at the implantation site, supported by local and circulating factors that support normal mammalian physiology. After a tumour growth period, teratomas are

removed and analysed through histopathological and other analytical assays for the presence of the three germ layers (Brivanlou & Rossant, 2003).

1.1.3 Ethical and Controversial Concerns

While the successful derivation of human ESCs opened doors to multiple research opportunities, it did not void ethical questions and dilemmas. Isolation of embryonic stem cells results in the destruction of the blastocyst and, ultimately, the death of an embryo. The ethical issue of ESC derivation, to this day, raises debates and arguments within the scientific community on whether pre-implantation embryos deserve the same considerations as post-implantation embryos. Advocates for the respect of human life are often at odds with those who believe that it is more important to uphold the duty of scientific advancement that can yield treatments and/or cures for ill patients (Mclaren, 2001).

1.2 Signaling Cascades Regulating mESCs

1.2.1 LIF/JAK STAT Signaling

One of the first methods used to maintain ESCs in an undifferentiated state was to grow them on feeder cell cultures, which produce a cytokine that inhibits differentiation called leukemia inhibitory factor (LIF). LIF acts by binding to LIF-receptor (LIF-R) and initiating its dimerization with gp130. A family of tyrosine kinases known as JAKs bind to the gp130 and LIF-R and auto-phosphorylate one another upon dimerization, which results in the recruitment and phosphorylation of signal transducer and activator of transcription factor 3 (STAT3). STAT3 forms a homodimer and translocates into the nucleus where it activates pluripotency genes such as *Oct4*, *Sox2* and *Nanog* (Boeuf, Hauss, De Graeve, Baran, & Kedinger, 1997; Matsuda et al., 1999). LIF primarily

inhibits mesendodermal differentiation (Wilson & Hemmati-brivanlou, 1995; Ying et al., 2008).

1.2.2 BMP4/SMAD Signaling

LIF alone is insufficient to maintain ESC pluripotency and leads to neuroectoderm differentiation of ESCs. To stimulate additional signalling, serum is incorporated in cell culture medium supplemented with LIF to maintain pluripotency. Specifically, within serum, BMP4, a member of the transforming growth factor β (TGFβ) family, utilizes the SMAD signaling pathway to drive expression of differentiation inhibitor genes. Mechanistically, BMP4 ligand binding initiates the heterotetramerization of serine kinase receptors known as BMPR1 and BMPR2 (Wang et al., 2014). BMPR1 and BMPR2 then phosphorylate Smad-1, Smad-5, and Smad8 which facilitates their translocation into the nucleus to activate inhibitor of differentiation (*Id*) genes. Neural differentiation is then suppressed by the binding of Id proteins to pro-neural basic helix-loop-helix (bHLH) factors (Ying et al., 2003). In a non-canonical fashion, BMP4 is further able to inhibit differentiation by suppressing the ERK1/2 and P38 mitogen-activated protein kinase (MAPK) pathways (Qi et al., 2004).

1.2.3 Wnt/β-catenin Signaling

The Wnt/β-catenin signaling pathway has three key components: the signal-initiating Wnt ligands, the effector protein-β-catenin, and the β-catenin destruction complex, which regulates the levels of cytosolic β-catenin (Gottardi & Peifer, 2008). In the absence of Wnt signalling, β-catenin levels are regulated to low levels by a cytoplasmic destruction complex which is formed, minimally, by AXIN, APC, GSK3, and CK1. Wnt ligand bound to cell membrane receptor Frizzled activates Wnt/β-catenin signalling, effectively

inactivating the β-catenin destruction complex. In the absence of a functional destruction complex, β-catenin levels increase in the cytoplasm, allowing it to translocate into the nucleus (Kimelman & Xu, 2006). Inside the nucleus, β-catenin influences the functionality of a family of TCF/LEF (T-Cell Factor/Leukemia Enhancing Factor) proteins to activate multiple Wnt target genes that support pluripotency (Lu, 2010).

1.3 Naive vs. Primed States of Pluripotency

Naive pluripotent stem cells represent preimplantation mouse blastocyst inner cell mass (ICM), whereas primed pluripotent stem cells represent post implantation epiblast cells. The different states of pluripotency have been linked to different states of epigenetic regulation of key pluripotency genes. Furthermore, naive pluripotent stem cells can contribute to blastocyst chimeras while their primed counterparts cannot (Nichols & Smith, 2009). Naive pluripotent stem cells such as mESCs tend to maintain self-renewal capacity upon Wnt signalling, while primed pluripotent stem cells rapidly differentiate (Takahashi, Kobayashi, & Hiratani, 2018).

1.4 Wnt/β-catenin (Canonical) Signaling Pathway (Detailed)

1.4.1 Wnt Off State

In the absence of secreted Wnt ligands, an assembly of proteins known as the β-catenin destruction complex actively degrades the Wnt effector β-catenin. The β-catenin destruction complex consists of AXIN, Adenomatous polyposis coli (APC), glycogen synthase kinase 3 (GSK3) and casein kinase 1 (CK1). The complex is held together through the Axin-APC scaffold, while GSK3 and CK1 contribute to the phosphorylation of β-catenin at Ser33/Ser37/Thr41 and Ser45, respectively (Zeng et al., 2005). The phosphorylation of β-catenin is sequential, as the CK1-mediated Ser45 phosphorylation

primes the subsequent Ser33/Ser37/Thr41 GSK3-mediated phosphorylation (Liu et al., 2002). Ser33/Ser37 phosphorylation of β-catenin specifically targets it for ubiquitination by β-TrCP and sequential proteasomal degradation (Winston et al., 2008). With an intact β-catenin destruction complex, β-catenin is destabilized, and its cytoplasmic levels are low. Within the nucleus, Wnt target genes are repressed by the TCF/LEF family of transcription factors bound to histone deacetylase (HDAC), and transducin-like enhancer protein (TLE) corepressors (Chodaparambil et al., 2014).

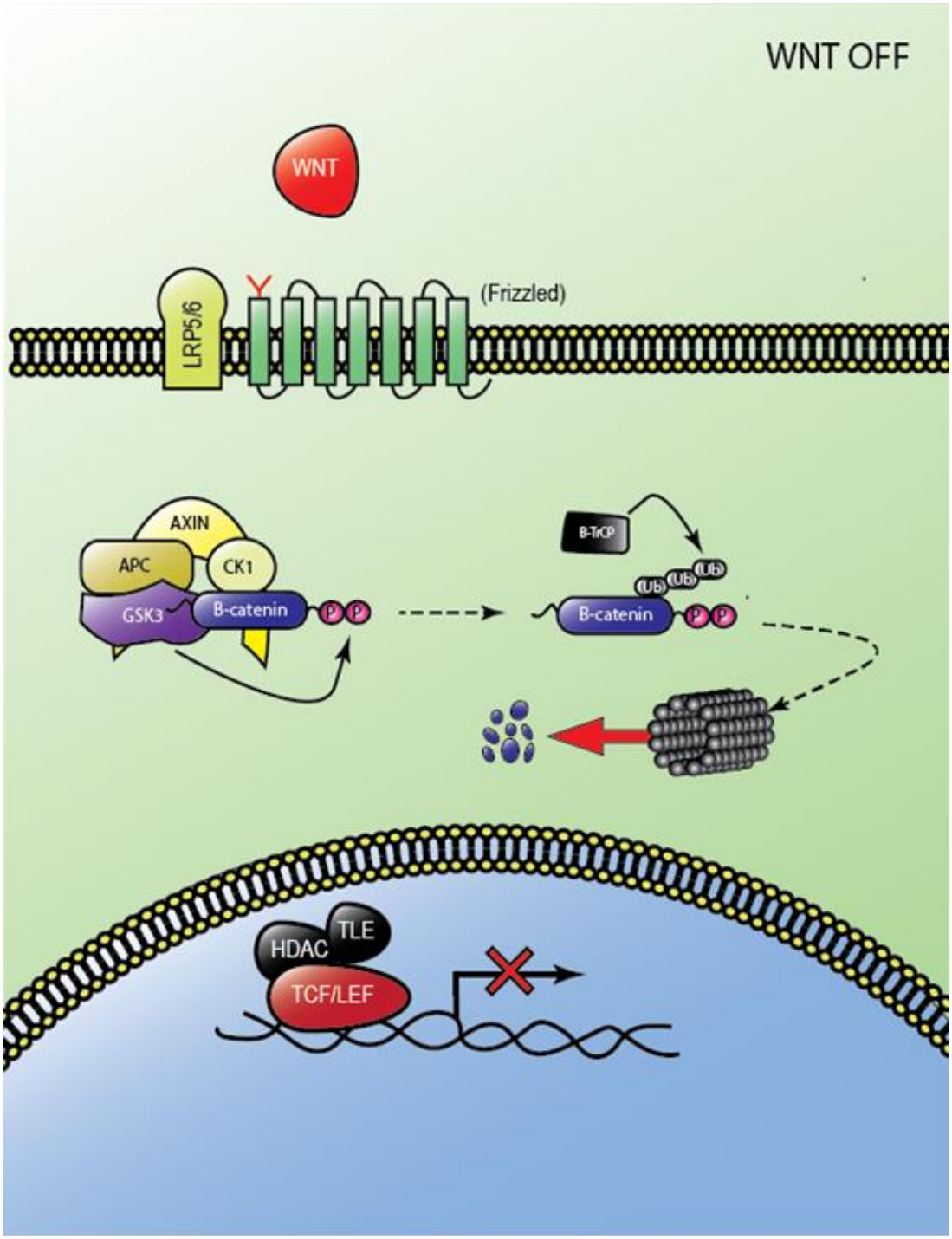

Figure 1. Mechanism of Wnt Signaling-WNT OFF.
In the absence of a Wnt ligand, AXIN, APC, CK1, and GSK3 form a complex, which facilitates the GSK3 dependent phosphorylation of β-catenin. Phosphorylated β-catenin is targeted by β-TrCP for ubiquitination-mediated proteasomal degradation. In the nucleus, Wnt target genes are repressed by the TCF/LEF family of transcription factors along with co-repressors, HDAC and TLE.

1.4.2 Wnt ON State

The Wnt signaling cascade is activated upon binding of a Wnt ligand to the N-terminal cysteine-rich domain of a GPCR receptor, Frizzled, and Lipoprotein receptor-related protein 5/6 (LRP5/6), which may induce the complex formation between the two Wnt associated receptors (He, 2004; Vldl et al., 2000). The Frizzled-LRP5/6 complex initiates the phosphorylation of an intracellular domain of LRP5/6 at five conserved PPP(S/T)PX(S/T) motifs. This phosphorylated motif produces a favorable binding site for Wnt negative regulator, Axin. Axin is then recruited and bound to the LRP5/6 tail (Rao & Kühl, 2010; Tamai et al., 2004; Zeng et al., 2005). Axin, as a crucial scaffold protein, co-translocates Ck1, and GSK3, compromising the β-catenin destruction complex. Wnt-activated Dsh promotes phosphorylation of GSK3 and prevents Ser33/Ser37/Thr41-phosphorylation of β-catenin. This leads to the stabilization of β-catenin and allows accumulation in the cytoplasm and ultimately translocation into the

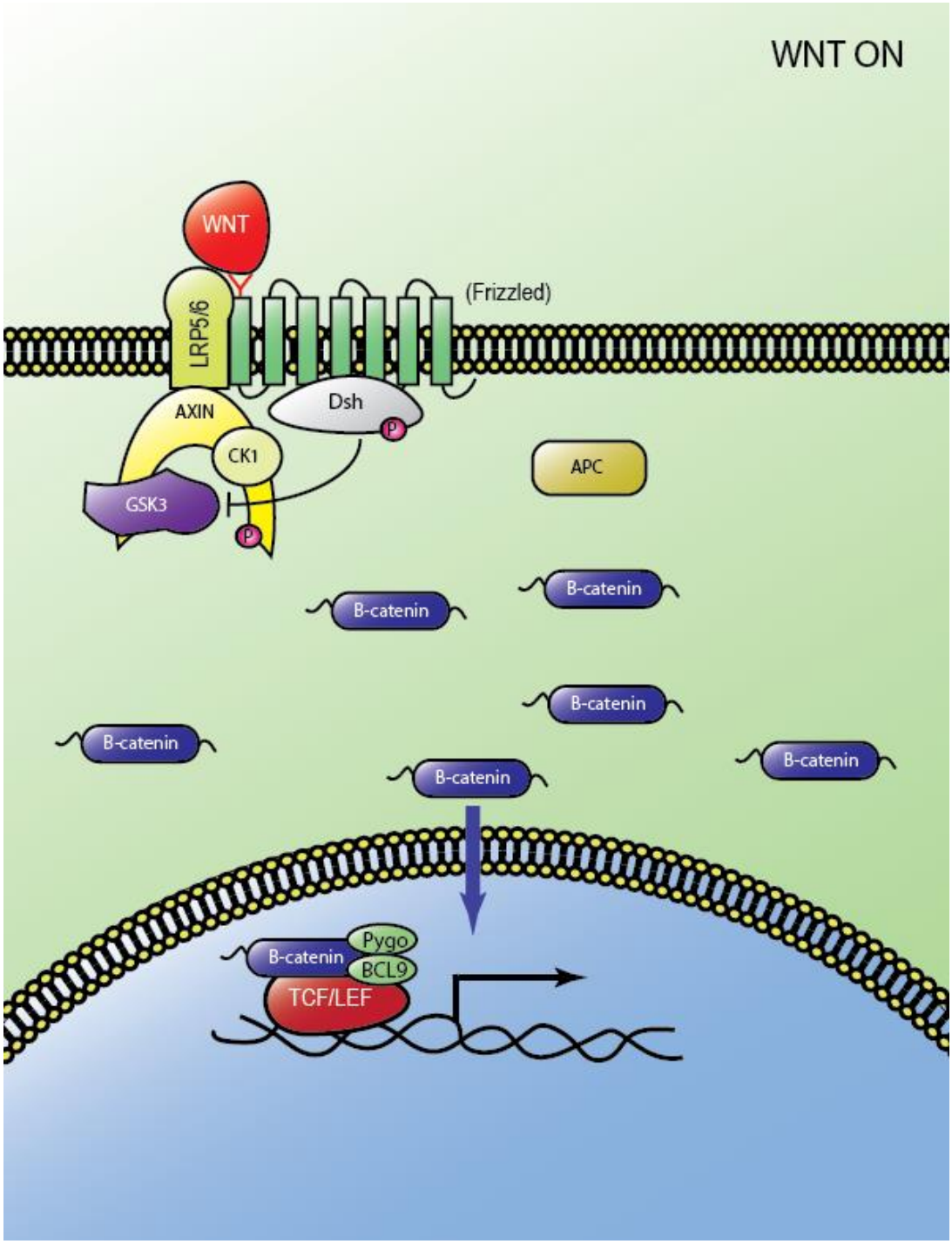

Figure 2. Mechanism of Wnt Signaling-WNT ON.
Wnt ligand binding to Wnt-receptor, Frizzled, induces dimerization with LRP5/6. The β-catenin destruction complex is compromised and localizes to the tail of LRP5/6, where activated Dsh prevents GSK3 phosphorylation of β-catenin. β-catenin accumulates in the cytoplasm and translocates into the nucleus, where it is bound by TCF/LEF and recruits co-activators to activate Wnt target genes.

nucleus through a poorly understood mechanism. Nuclear β-catenin binds to the β-catenin binding domain of TCF/LEFs and initiates the formation of a TCF/LEF activating complex by changing the conformation of DNA-bound TCF/LEF and recruiting co-activators such as Pygo and BCL9 (Kramps et al., 2002).

1.4.3 TCF/LEF Family of Transcription Factors

In invertebrates, a single TCF carries out the dual functions of gene activation and repression, whereas vertebrates express four family members, LEF1, TCF7 (also known as TCF1 in older literature), TCF7L1 (also known as TCF3 in older literature), and TCF7L2 (also known as TCF4 in older literature) (Cadigan & Waterman, 2012). Each TCF has five different conserved regions that support its function as a transcription factor downstream of Wnt signaling. The β-catenin binding domain binds β-catenin and turns TCF into an activator of Wnt target genes. The Groucho/TLE binding site binds to the glutamine-rich Q domain of Groucho or TLE (vertebrate) corepressors to suppress Wnt target genes (Daniels & Weis, 2005). The HMG domain binds the minor groove of the DNA helix at the consensus sequence, 5'-ACATCAAAG-3', called the Wnt response element, and induces a 90°-127° bend that allows linearly distant transcription factors to be brought closer together (Giese, Kingsley, Kirshner, & Grosschedl, 1995).

TCF factors are localized to the nucleus and bind DNA through a basic tail domain located close to the C-terminus of the HMG domain, which also acts as a nuclear localization sequence. The C-clamp is a small domain near the HMG domain that also binds to GC rich regions of DNA known as "helper sites" (Atcha et al., 2007; Gris, 2008).

TCF specialization is observed in vertebrates through alternative promoter usage and alternative mRNA splicing, which result in the expression of several TCFs with

individualized properties (Vacik & Lemke, 2011). Although all members of the TCF/LEF family share distinctive functional domains, LEF1 and TCF7L1 function as an activator and a repressor respectively, while TCF7 and TCF7L2 have context dependent regulatory functions (F., O., & S., 2005; Kim, Oda, Itoh, & Chitnis, 2000).

1.4.4 Stimulator of Wnt Signaling

Amplifying and increasing sensitivity of Wnt signaling activation is a family of secreted proteins, R-Spondins. In the absence of R-Spondins, the Wnt receptor Frizzled is targeted for degradation by RNF43 and ZNRF3 E3 ubiquitinases. R-Spondin "cross-links" RNF43/ZNRF3 to the LGR5/6 receptor, and the resulting ternary complex is quickly endocytosed, thereby enhancing Wnt responsiveness due to a higher number of Wnt-responsive-Frizzled receptors (Lau, Peng, Piet, & Clevers, 2014). R-spondin has a dynamic expression pattern during embryogenesis, providing a rationale for its importance in certain key steps during development requiring elevated Wnt signaling (Nam, Turcotte, & Yoon, 2007).

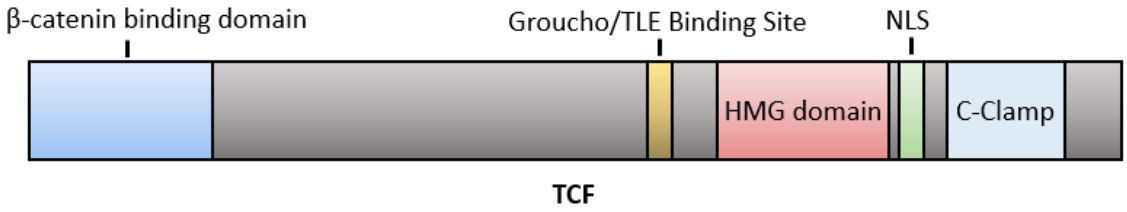

Figure 3. Conserved domains of invertebrate TCF.
5 different domains exist for TCFs including the β-catenin binding domain, Groucho/TLE binding site, DNA binding HMG domain, nucleus localization sequence-basic tail, and the C-clamp.

1.5 Wnt Signaling in Development and Adult Tissue Homeostasis

Embryonic development of multicellular organisms requires precise cell-cell communication to ensure coordinated cell fate decisions, self-renewal, cell migration and

cell to tissue organization. The evolutionarily conserved Wnt signaling pathway is an indispensable communication mechanism that closely orchestrates development in metazoan systems. Proper gradients of Wnt signaling are crucial in defining the anteroposterior and dorsoventral body axes of an organism to establish the organism's architecture (Genikhovich & Technau, 2017; Niehrs, 2010). Differences in regional Wnt-stabilized β-catenin can define cell populations/compartmentalization and induce posterior formation cooperatively with BMP signaling, by forming organizing centers.

A Wnt-β-catenin signaling gradient is established in post-gastrulation vertebrate embryos, with high Wnt-β-catenin signaling at the posterior and inhibited Wnt- β-catenin signaling at the anterior. This leads to the development of head structures at the anterior and tail structures at the posterior (Green, Whitener, Mohanty, & Lekven, 2015). During earlier *Xenopus* embryo development, the blastula defines its ventral-dorsal axis through a Wnt β-catenin signaling gradient. High nuclear β-catenin is observed at the dorsal side and minimal-to-no nuclear β-catenin is detected on the ventral side (Moon & Kimelman, 1998). Post full development of the embryo, Wnt signaling remains vital to facilitate tissue homeostasis in most organ systems, and its impact on intestine, bone, and hair follicle stem cells has been well characterized.

1.5.1 Intestine

The intestine connects the stomach to the rectum, functioning to absorb nutrients, minerals and water from digested food particles. To effectively carry out its primary function of absorption, the inner surface of the intestine has a folded structure which increases surface area and regulates flow of digested food. Individual folds have projections called villi which carry out absorption and generate secretions. The epithelial layer of the intestinal

fold creates two distinct structures, the previously mentioned villi at the apex of the fold and the crypts at the base. The crypts house highly proliferative progenitor cells that migrate to the villi through the influence of multiple cellular signaling events, prior to undergoing apoptosis. A Wnt signaling gradient is established between the crypts and the villi, where Wnt ligands and R-spondins are secreted by myofibroblast cells to promote self-renewal of CBC progenitors located in the crypts (Kabiri et al., 2014). As CBC progenitors divide away from the Wnt source crypts, they lose the ability of self-renewal and differentiate into a variety of intestinal cell types with different functions.

1.5.2 Bone

A Wnt co-receptor, LRP5 (Low-Density Lipoprotein Receptor-Related Protein 5), is indispensable for proper bone tissue maintenance. LRP5 loss of function mutations causally lead to osteoporosis-pseudo glioma syndrome, a low bone mass disorder (Gong et al., 2001). At the cellular level, optimal bone remodeling occurs through the action of three different bone cell types to meet the mechanical demands of a skeleton and systemic calcium homeostasis. Osteoclasts are responsible for bone resorption and lead to decreased bone mass (Zhang et al., 2000). Osteoblasts increase bone density by bone matrix formation and are differentiated from mesenchymal progenitor cells by the binding of Wnt ligands to a functional LRP5 Wnt co-receptor (Cui, Y. Niziolek, P. MacDonald, 2011; Pittenger et al., 1999). Osteocytes regulate osteoblast differentiation by the release of Wnt ligands and sclerostin (encoded by the *SOST* gene), which inhibits LRP5 receptors to reduce osteoblast formation. *SOST*-loss of function, and *SOST* expression-decreasing mutation studies describe pathologically increased bone mass (Balemans et al., 2002; Brunkow et al., 2001; Loots et al., 2005), and prompted scientists to consider

therapeutically augmenting bone mass by using antibodies directed against sclerostin (Glorieux et al., 2017; Recker et al., 2015).

1.5.3 Hair Follicle

The mammalian hair follicle undergoes a cycle of telogen (rest), anagen (growth), and catagen (degeneration). During the telogen phase, hair follicle stem cells (HFSC) reside in the bulge region of the hair follicle, where they slowly cycle and depend on low levels of autocrine-Wnt for maintenance (Cotsarelis, Sun, & Lavker, 1990; Lim, Tan, Yu, Lim, & Nusse, 2016). Elevated Wnt signaling induces the telogen-anagen transition and facilitates the migration of HFSC toward the base of the hair follicle, where they rapidly proliferate to generate cells of hair follicles (Oshima, Rochat, Kedzia, Kobayashi, & Barrandon, 2001; Tumbar et al., 2004).

1.6 Insights into the Mechanisms of TCF/LEF Function

A commonly accepted mechanism of Wnt gene regulation by the TCF/LEFs is that TLE corepressor-bound TCF/LEFs act as gene repressors, while Wnt-induced β-catenin-bound TCF/LEFs act as gene activators. The transcriptional switch induced by the swapping of β-catenin and TLE oversimplifies nuclear Wnt signalling, and further studies have added complexity to the transcriptional theory.

1.6.1 TCF/LEF-TLE Repression is not Universally Observed

Franz and colleagues have shown that TCF-mediated repression of Wnt targets is not a universal phenomenon, by showing that only 37.5% Wnt target genes were significantly derepressed upon Pan (*Drosophila* TCF/LEF) absence in unstimulated *Drosophila* cell lines.

1.6.2 β-catenin/TLE Co-regulator Switch versus Conformational Switch

It is accepted that β-catenin can facilitate Wnt target activation through the recruitment of a transcriptional co-activator complex consisting of B-cell CLL/lymphoma 9 (Bcl9), and Pygopus 1/2 (Pygo) (Cadigan, 2012). Interestingly, it has been shown by different groups that the co-repressor, TLE also interacts with Bcl9 in HEK293 cells, and Pygo in *Drosophila*. Regardless of Wnt stimulation state, co-IP experiments were able to show that TCF/LEFs were complexed with Bcl9/Pygo, challenging the β-catenin /TLE switch theory. As an alternative, the authors suggested that upon Wnt signaling, β-catenin binding induces a change in conformation instead of TLE displacement (van Tienen, Mieszczanek, Fiedler, Rutherford, & Bienz, 2017).

1.6.3 Wnt Induced TLE3 Ubiquitination Facilitates a Transcriptional Switch

A major gap in the TCF/LEF transcriptional switch mechanism was filled through the identification of TLE3 ubiquitination on its C-terminal WD40 domain by E3 ubiquitin-protein ligase (UBR5) (Flack, Mieszczanek, Novcic, & Bienz, 2017). Upon Wnt signaling, UBR5 creates a K48-linked polyubiquitin chain on TLE3 (Wolf & Hilt, 2004), increasing affinity to protein unfolding Valosin-containing protein (VCP) (D, Tang, & Y, 2016). VCP, through its ATPase activity, is suggested to disrupt the tetramerization of ubiquitinated TLE3 required to repress Wnt targets (Chodaparambil et al., 2014).

1.6.4 TCF7L1: Dedicated Transcriptional Repressor or Functionally Redundant Activator?

Unlike invertebrates, which contain one TCF that facilitates both activation and repression of Wnt target genes, vertebrates contain multiple TCF/LEFs (Cadigan, 2012). This generated questions of redundancy and specialization of individual TCF/LEFs and prompted researchers to believe that TCF7L1 is a dedicated repressor. In mouse embryonic

stem cells (mESCs), TCF7 and TCF7L1 have been shown to have opposing functions, as TCF7 activates, and TCF7L1 represses, the same transcriptional targets (Yi et al., 2012).

Moreira et al, challenged the TCF7-TCF7L1 antagonistic relationship by showing the capacity of TCF7L1 to take over the activating function of TCF7 by rescuing gene expression and differentiation defects upon reintroduction of TCF7 or TCF7L1 at its endogenous genomic locus (Moreira et al., 2017). These results further challenge the generally accepted idea of TCF/LEF dedicated regulatory function and suggest that TCF/LEFs may have redundant capabilities to mutually accommodate expression of important genes.

1.7 Genes and Proteins of Interest

1.7.1 Sall4 (Spalt like-4)

Sall4, belongs to a family of Spalt-like (SALL) transcription factors that plays a crucial role in embryonic stem cells, pluripotency and differentiation. Sall4 is a key ESC factor that binds to Nanog, Sox2 and Oct4, the essential stem cell transcription factors regulating pluripotency. (Pardo et al., 2010; van den Berg et al., 2010). Together, these proteins form a regulatory network by affecting the expression pattern of each other and themselves (Kim, Chu, Shen, Wang, & Orkin, 2008).

Sall4 enhances the transcription of *Pou51,* which encodes for Oct4, by binding to a highly conserved region of the *Pou51* distal enhancer and promoting its expression. miRNA suppression or knockout (KO) of SALL4 in mESC leads to differentiation up to the trophoblast lineage and a significant increase in CDX2 expression, a marker of differentiation (Zhang et al., 2006). Through alternative splicing, Sall4 carries out unique functions in ESCs as isoforms A, B and C. Sall4a and Sall4b, most heavily studied, form

hetero- and homodimers with each other to bind and regulate different regions of the DNA while establishing different sets of protein-protein interactions.

The isoforms of SALL4 vary in size ranging from 113kd, 66kd, and 30kd (a, b, and c isoforms, respectively) and carry out overlapping and unique functions. A conserved N-terminal 12 amino acid (N-12aa) domain shared by all isoforms of SALL4 conducts transcriptional repression by recruiting the NurD complex, comprising subunits that include HDAC1/2 and histone chaperones RbAp46/48 (Lauberth & Rauchman, 2006). In context relevant to Wnt signaling, Kohlhase J and colleagues (2006) reported the regulation of Sall4 by canonical Wnt signaling at the transcriptional level and described the presence of a TCF/LEF consensus sequence within the promoter of Sall4. Quantified through a luciferase reporter assay, mutation of the TCF/LEF-binding site by using site-directed mutagenesis strongly decreased the promoter's activity by 36%, supporting an extensive role of TCF/LEF transcription factors in promoting effective transcription of Sall4 (Böhm, Sustmann, Wilhelm, & Kohlhase, 2006).

Sall4 has been shown to interact with β-catenin through co-immunoprecipitation, as has the transcriptional family member Sall1. Although the interaction domain between SALL4 and β-catenin is not fully defined, binding data of SALL1 and β-catenin suggest that the interaction most likely involves the C-terminal region of SALL4 (Sato et al., 2004).

1.7.2 Jmjd1c (Jumonji Domain Containing 1-c)

JMJD1C is an H3K9 histone demethylase that is known to play a role in DNA damage repair, spermatogenesis, and the activation of key transcription factors. JMJD1C interacts with thyroid hormone nuclear receptors, potentially through its jumonji domain. JMJD1C has been reported to be one of the most upregulated genes in leukemia and serves to

perpetuate the self-renewal capacity of cancerous hematopoietic stem cells (Bedford et al., 2000). Based on a transcriptomic database of human embryonic stem cells (hESC), pluripotency states have been strongly correlated with high levels of JMJD1C (Roux, Kim, Raida, & Burke, 2012). JMJD1C is abundantly expressed in naïve pluripotent states and gradually declines during differentiation in response to signalling pathways such as BMP signalling activation (Xu et al., 2008).

JMJD1C was first suggested to play a role in the pluripotent circuitry of stem cells as a downstream gene target, after a putative OCT4 binding site was identified in its promoter (Katoh & Katoh, 2007). Mechanistically, Wang and colleagues (2014) reported the crucial role of JMJD1C-mediated epigenetic regulation of miR-302 that strongly supports the JMJD1C pluripotency maintenance theory. JMJD1C knockdown (KD) cells demonstrated the downregulation of miR-302, which associates with OCT4 and functions as a neural repressor during differentiation. JMJD1C KD resulted in ESCs differentiating into neural progenitors after 3 days, much faster than wild type controls in similar conditions of FGF signalling inhibition used to promote initiation of neural differentiation (J. Wang, Park, Drissi, Wang, & Xu, 2014). In addition, JMJD1C has been reported to interact with another pluripotency factor, KLF4, to maintain ESC identity by suppression of EMT and differentiation signalling pathways such as ERK/MAPK signalling (Xiao et al., 2017). It is evident that JMJD1C has a significant influence in stem cell biology and cancer. It may also play an important role in the Wnt/β-catenin pathway that is yet to be reported.

1.7.3 SMARCA4 (SWI/SNF-Related Matrix-Associated Actin-Dependent Regulator)

Brahma-related gene 1 (*Brg1*), as a member of the SWI/SNF family of proteins, regulates the transcription of target genes in a chromatin altering manner, through its helicase and

ATPase activities. The protein expressed from the *Brg1* gene, SMARCA4, has important implications in the proper development of mammalian organisms, particularly in development past the pre-implantation stage. Cancer patients with a SMARCA4 mutation display a high preference for missense mutations that are commonly discovered in the conserved ATPase domain (Stanton et al., 2017). These mutated ATPase domains are thought to disrupt enhancer accessibility at thousands of genomic sites (Courtney Hodges et al., 2018). Interestingly, SMARCA4 also interacts with β-catenin, although it remains to be elucidated whether this interaction is direct or, potentially, TCF/LEF mediated.

1.7.4 Tbx3 (Tbox-3)

Tbox-3 (Tbx3) belongs to a subfamily of T-box transcription factors known to bind DNA at consensus sites called T-box binding elements. Tbx3 has been implicated in tissue development, notably of the mammary gland (Chapman, Garvey, et al., 1996). Tbx3 is expressed early in the blastocyst, then subsequently in the limbs, lung mesenchyme, and mammary gland. Tbx3-mutations have been shown to cause Ulnar-mammary syndrome, affecting limb, tooth, hair, genital, and apocrine gland development (Koboldt et al., 2012). Tbx3 contains a highly conserved repressive domain, that represses tumor supressors p14/p19 ARF by interacting with histone deacetylases. Therefore, overexpression of Tbx3 has implications within breast cancer and the inhibition of senescence (Koboldt et al., 2012). Tbx3 is a known Wnt target gene, physically bound and activated by β-catenin and TCF7L2, as determined by ChIP. In murine liver tumors and human hepatocellular carcinomas, mutated status of β-catenin is heavily associated with overexpression of Tbx3 (Renard et al., 2007).

PROJECT RATIONALE

The Wnt pathway is a highly complex metazoan signaling mechanism that is indispensable for proper development, with disease causing consequences upon deregulation. Its complexity stems from an abundance of unknown interactions and the interplay of multiple genes and proteins that must be elucidated to effectively manipulate core signaling mechanisms for the development of new therapeutic agents. In this thesis, we cover the elucidation of novel protein interactors of TCF7L1, the most abundantly expressed member of the TCF/LEFs in mESCs at transcript and protein levels. Changes in gene expression patterns being the ultimate consequence of Wnt signaling, identification of TCF7L1 interacting proteins may provide insights into how TCF7L1 activates or represses gene targets. In addition, uncovering specific gene targets that are regulated by distinct complexes of TCF/LEFs containing different proteins, may allow for strategic interventions to therapeutically correct expression levels of specific gene subsets.

HYPOTHESES

1. Genuine protein interactors of TCF7L1 can be identified through the Bio-ID assay and therefore can be validated by using Co-IP and PLA.
2. TCF7L1 works closely, and in concert with, multiple proteins of different gene ontologies to regulate Wnt target gene expression.
3. SALL4 can modulate the function of ‘dominant-negative’ TCF/LEFs lacking an N-terminal β-catenin binding domain.

CHAPTER 2: MATERIALS AND METHODS

2.1 Cell culture

mESCs were cultured on 0.1% gelatin-coated plates supplemented with mESC-supporting medium (Dulbecco's Modified Eagle Medium, non-essential amino acids, sodium pyruvate, glutamate; (all from Thermo Fisher), 2-mercaptoethanol (Sigma), and LIF (Amsbio). At 80% cell population confluency, cells were rinsed with Dulbecco Phosphate Buffered Saline (DPBS) and separated with Accutase (Sigma) and passaged at a 1/8 split ratio. Cells were passaged every 2-3 days and grown in a 37℃, 5% CO2 incubator.

2.2 Transfection

Transfection reagent Lipofectamine 2000 (Invitrogen) was utilized to deliver target plasmids into mESCs. 2 million mESCs were transfected with 2 µg of DNA and 4 µL of Lipofectamine. Lipofectamine and DNA were individually incubated with 100 µL OptiMEM (Thermo Fisher) for 5 minutes. Lipofectamine and DNA were combined and allowed to incubate for an additional 20 minutes, all at room temperature. Cells were harvested from the plates with Accutase (Sigma) and resuspended in OptiMEM and pelleted after centrifugation at 244 x g for 3 minutes. The cells were resuspended in Lipofectamine-DNA-OptiMEM mixture, plated accordingly, and grown in standard cell culture methods as previously mentioned.

2.3 Gene Cloning/PCR

Following instructions listed in the In-Fusion HD Cloning Kit (Thermo Fisher), PCR-amplified target insert flanked with 15 bp homology sequences were cloned into their appropriate backbone vector.

Generation of pE1F1-JMJD1C-V5

JMDJ1C was PCR-amplified from PCR-XL-TOPO-Jmjd1c by using PrimeStar MAX PCR mix and In-Fusion-cloned into KpnI and BstBI digested pEF/FRT5_TOPO-MAxin2(V5).

Generation of pCMV-TCF7L1-3xFLAG

TCF7L1 was PCR-amplified from pCMV-SPORT6-TCF7L1 by using PrimeStar MAX PCR mix and In-Fusion-cloned into BamHI and HindIII digested p3xFLAG-CMV-14.

Generation of pCMV-SALL4-3xFLAG

SALL4 was PCR-amplified from pAsx-SALL4 by using Primestar MAX PCR mix and In-Fusion-cloned into ClaI and BamHI digested p3xFLAG-CMV-14.

2.4 Dual-Luciferase Reporter Assay

HEK293T cells were transfected following the previously mentioned method, with pM50-8xTOP, pRL-CMV, and control vector/overexpression plasmid. 20 000 transfected cells were seeded onto a 96-well plate and incubated for 24 hours in 37°C/5% CO_2. Cells were washed with PBS and then lysed over 20 minutes in Passive Lysis Buffer while shaking. Cell lysates were transferred onto an opaque 96-well plate and were combined with reporter assay reagents-LARII and Stop/Glow (Promega). Relative luciferase activity was quantitatively measured using a FLUOstar OMEGA instrument with subsequent analysis in Microsoft Excel.

2.5 Generation of mESCs stably overexpressing Sall4

E14TG2A mESCs were transfected by using the previously described protocol, with pCMV-SALL4-3xFLAG and pCAG-MKO2-Puro selectable marker. Transfected cells

were plated at low density (50 000 cells per 10 cm culture plate) and incubated in 37°C, 5% CO_2 for 48 hours. Transfected cells were selected for puromycin resistance in mESC medium containing 1 µg/mL puromycin for two weeks, with fresh medium replenishment every 3 days. Puromycin-resistant colonies were picked under a microscope by using a pipettor set to 10 µL, were disaggregated by using Accutase (Sigma), and were plated into wells of a 96-well plate containing medium supplemented with 0.5 µg/mL puromycin. Colonies were then expanded onto 24-well, 12-well, and finally 6-well plates prior to western blot analysis.

2.6 Proximity Ligation Assay

70 000 cells were plated per well of an Ibidi µ-slide 8-well chamber slide and were allowed to grow to 80% cell confluency. Individual wells were rinsed with 37°C PBS and fixed with 4% formaldehyde (Sigma) for 10 minutes at room temperature. Cells were sequentially fixed and permeabilized with 70% methanol for 5 minutes and were washed once more with PBS. Cells were blocked with blocking solution provided with the Duolink in situ red kit (Sigma) for 30 minutes at 37°C and were then incubated with primary antibodies at a 1:1000 dilution overnight at 4°C. After two sequential wash steps with Wash Buffer A, cells were incubated with PLA probes at 37°C for 1 hour. After two sequential wash steps with Buffer A, ligation mixture was added and allowed to further incubate for 30 minutes at 37 °C. After two sequential wash steps with Buffer A, cells were incubated in amplification-polymerase solution for 100 minutes at 37°C. Finally, cells were washed three times with Wash Buffer B and were imaged by using confocal microscopy.

2.7 RNA Extraction

At approximately 70% cell confluency on a 60 mm plate, 1 million cells were harvested by using the cell disaggregation solution, Accutase (Sigma). Pipettes and work benchtop were wiped down with RNase Zap solution (Sigma) prior to RNA purification. Cells were washed once with 1X PBS and were then processed for RNA purification by using Monarch Total RNA Miniprep Kit (NEB). Purified RNA was stored until further use at -80°C and re-quantified after every thaw by using a Spectrophotometer 1000.

2.8 Reverse Transcription/cDNA Synthesis

LunaScript RT Supermix (NEB) was used to reverse transcribe RNA into cDNA by following kit instructions. cDNA synthesis was carried out by using the following temperature settings: 25°C for 2 minutes, 55°C for 10 minutes, and 95°C for 1 minute. cDNA was stored at -20°C prior to use.

2.9 qPCR/RT-qPCR

Individual wells of a 96-well qPCR plate (Thermofisher) contained 20 µL volumes of qPCR reactions consisting of: 10 µL Lunascript qPCR mastermix (NEB), 1 µL reverse/forward qPCR primers (10 µM stocks), 2 µL cDNA, and 7 µL water. Microamp plates were sealed with a Bio-Rad qPCR sealer and centrifuged at 425 x g for 1 minute.

2.10 Co-Immunoprecipitation

All Co-IP experiments were performed by using the Dynabeads™ Co-Immunoprecipitation Kit (Invitrogen). Following the protocol outlined in the kit, 1.5 mg Dynabeads M-270 Epoxy were coupled to 7 µg M2-FLAG antibody (Sigma F1805) or 5 µg β-catenin antibody (BD Transduction 610154). 500 µg protein in 250 µL lysis buffer was incubated with FLAG antibody-coupled Dynabeads for 1 hour at 4°C on a rotator. Dynabeads were washed three times with 200 µL of cell lysis buffer and once more with

wash buffer provided in the kit. Antigen was eluted in 30 µL EB Elution buffer with hand-agitation for 5 minutes. For re-CoIP experiments, initial FLAG-IPs were performed in duplicates to obtain a total of 60 µL of eluted FLAG antigen protein. Half of the eluate was further probed for β-catenin after topping up to 750 µL in lysis buffer and resuspending in β-catenin antibody-Dynabeads. Dynabeads were washed three times with 200 µL cell lysis buffer and once more with wash buffer provided in the kit. Antigen was eluted in 30 µL of EB Elution buffer with hand-agitation for 5 minutes. IP protein samples were added to 3X LDS sample buffer containing Bond-Breaker TCEP (Thermo Fisher) and heated at 65°C for 5 minutes prior to western blotting.

2.11 Chromatin-Immunoprecipitation-qPCR

Experimentally validated promoter sequences of Tbx3 were obtained from the Eukaryotic Promoter Database (https://epd.epfl.ch//index.php) and were screened for TCF/LEF binding motifs on JASPAR (jaspar.genereg.net). Genomic DNA sequencing primers flanking the predicted TCF/LEF binding motifs were designed by using the NCBI-PRIMER BLAST tool with the parameters of 70-150 bp PCR product size and 400 bp genetic coverage region. Designed primers were purchased from IDT. 3xFLAG TCF3 mESCs were grown to 70-90% confluency on four 10 cm culture plates. One of the four plates was used as a cell count plate. The remaining plates were crosslinked with 1% formaldehyde added directly to the culture plate and quenched with glycine. After a PBS wash, cells were scrape-harvested into 15 mL-conical tubes. Nuclei fractions were isolated after subsequent lysis with Buffer A and Buffer B supplied with the kit. DNA was digested with Micrococcal Nuclease to approximately 150-900 bp and quenched with 0.5 M EDTA. Chromatin was further processed by sonication in ChIP Buffer with 3 sets of 20-sec 30%

amplitude pulses. Lysates were clarified via centrifugation and 50 µL was removed for chromatin digestion/concentration analysis. 10 µg digested, crosslinked chromatin preparations were probed with 2 µg FLAG antibody (Sigma F1809), Normal Rabbit IgG-negative control, or Histone H3 antibody-positive control overnight. 30 µL protein G magnetic beads were added to the lysate-antibody mix and further incubated for 2 hours at 4°C. The beads were thoroughly washed and eluted with ChIP elution buffer at 65°C for 30 minutes. Crosslinking was reversed by using 5M NaCl and Proteinase K for 2 hours at 65°C. Eluted DNA was purified from protein via spin columns and was then quantified by using qPCR.

Table 1. Tbx3 Promoter: ChIP-qPCR Primers

Primer	Sequence
Set 1(523-606)	FWD: 5'-ACGTTCCAGTTTCCGACACC-3' REV: 5'-GCTGCATAGGCGTGGTTTTC-3'
Set 2(563-635)	FWD: 5'-CTATTCCCCCAGCACTCGAC-3' REV: 5'-TCTTTGACGCTTTCGGACCA-3'
Set 3(774-864)	FWD: 5'-TCCCTCTACTTGCCTACTCC-3' REV: 5'- GGAGGATCAAGAAGACGGGT-3'
Set 4(1086-1185)	FWD: 5'-GGAAAGGGGCTTAAATCGCT-3' REV: 5'-GCTAGACTCTGGCTTTCAC-3'
Set 5(1517-1612)	FWD: 5'-TCTCTTCCCCCCAAAGACAC-3' REV: 5'-AAC AGCGACGCATAGTTTTG-3'

*ChIP qPCR Primer Sets- Mus musculus strain C57BL/6J chromosome 5, GRCm38.p4 (Promoter Region of Tbx3)

2.12 Western Blotting

10-20 µg protein samples were run on a 8%-10% bis-tris polyacrylamide gel at 160V for 60 minutes and were then wet transferred onto a polyvinylidene fluoride (PVDF)

membrane in Towbin's transfer buffer (25 mM Tris, 192 mM glycine, and 20% (v/v) methanol) at 200 mA for 2 hours. PVDF membrane was blocked in 5% skim milk/tris buffered saline (TBS) solution for 1 hour and incubated overnight with respective primary antibodies in 3% skim milk/TBS-TWEEN®20(TBS-T). After three sequential 5-minute PBS washes, PVDF membrane was probed with secondary antibody in 3% skim milk/TBS-T solution for 1 hour at a 1:20,000 dilution. Following an additional three washes, PVDF membrane was incubated in 25% Luminata Forte Western HRP Substrate (Millipore) solution for 5 minutes and was then imaged on a Chemi-Doc MP Imaging System (BioRad).

2.13 Preliminary Work on Protein Overexpression

2.13.1 Cloning SALL4-pMCSG7 and TCF7L1-pMCSG7

Tcf7l1 and Sall4 cDNA was PCR amplified by using the following primers listed in Table 2. Primer regions highlighted in red and blue are the stretches of DNA ends that permit compatibility for ligase-independent cloning (LIC) into a pMCSG7 vector.

Table 2. Primer Sets used to PCR amplify SALL4/TCF7L1 cDNA compatible with LIC into pMCSG7

Primer	Sequence
SALL4-MCSG7 Insert	FWD: 5'- TACTTCCAATCCAATGCAATGTCGAGGCGCAAGCAG-3' REV: 5'- TTATCCACTTCCAATGTTATCAGCTGACAGCAATCTTATTTTCC TCC-3'
TCF7L1-MCSG7 Insert	FWD: 5'- TACTTCCAATCCAATGCAATGCCCCAGCTCGGTGGTG-3' REV: 5'- TTATCCACTTCCAATGTTATCAGTGGGCAGACTTGGTGA CC -3'

The backbone, pMCSG7 plasmid was SSPI-digested for 6 hours at 37℃ and then purified with a PCR purification Kit. Simultaneously, the following reagents were added:

LIC PCR Preparation:
0.2 pmol SALL4/TCF7L1 PCR product
2 µL of 10X T4 DNA polymerase buffer (LIC Certified, Novagen)
1 µL of 100 mM DTT
2 µL of 25 mM dCTP
0.4 µL (1U) of T4 DNA polymerase (LIC Certified, Novagen)
dd$H_2$0 to 20 µL

LIC Vector Preparation:
100 ng of SSPI linearized pMCSG7
2 µL of 10X T4 DNA polymerase buffer (LIC certified, Novagen)
1 µL of 100 mM DTT
2 µL of 25 mM dGTP (same rules as above)
0.4 µL L (1U) of T4 DNA polymerase (LIC certified, Novagen)
dd$H_2$0 to 20 µL .

The reaction was incubated at 22℃ for 30 minutes, then heat deactivated at 70℃ for 20 minutes. The LIC PCR and vector preparations were combined and incubated at 70℃ for 2 minutes. The LIC reaction was then transformed into TOP10 cells.

2.13.2 IPTG induction testing

pMCSG7-SALL4/TCF7L1 constructs were transformed into BL21 and Rosetta2 competent cells overnight in 10 mL cultures. The next morning, 500 µL of overnight culture was inoculated into 100 ml LB and allowed to grow to OD600 of ~1. 500 µL of culture was pelleted and frozen down prior to induction as a "pre-induction" sample. Cultures were induced with 50 µL of 1 M IPTG (final concentration of 0.5 mM), and 500 µL samples were collected and pelleted at 1-hour, 2-hour, 3-hour, and overnight time points. Pellets were lysed in 50 µL of 2X LDS loading dye and heated at 95℃ for 10 minutes prior to loading on an SDS-PAGE gel. After gel electrophoresis, the polyacrylamide gel was

stained with 0.25% Coomassie Blue R-250 stain for 4 hours. The gels were destained overnight using 5% MeOH, 7.5% HoAC, 87.5% H_20-destaining solution.

CHAPTER 3: RESULTS

3.1 TCF7L1 interacts with JMJD1C, ARID1A, SMARCA4, and SALL4 as determined by PLA

The schematic of the PLA assay capturing protein-protein interactions is shown in Figure 4, where the interacting proteins act as the foundation for the PLA complex consisting of the primary antibody, secondary antibody-PLA probes, amplified DNA, and fluorescent probes. TCF7L1 was probed with FLAG antibody (F1805 Sigma) in mESCs with a 3xFLAG epitope knocked into the endogenous locus of TCF7L1. Through the proximity ligation assay, novel TCF7L1 interactors were validated. As negative controls, fixed cells were probed with a single antibody probing for one of the potentially interacting proteins. In addition, to test potential punctae enrichment as a sole result of two different IgGs of different animal origins, normal IgG rabbit and FLAG antibodies were also incorporated together. Incorporating only FLAG, JMJD1C, SMARCA4, or SALL4 antibodies did not produce visible punctae as determined through immunofluorescence. However, experimental parameters incorporating FLAG antibody with JMJD1C, ARID1A, SMARCA4, or SALL4 antibodies displayed an enrichment of punctae, suggesting protein-protein interactions (Figure 4).

3.2 Immunoprecipitation of TCF7L1 captures TCF7L1-SALL4 Interaction

As a second mode of validation, the TCF7L1-SALL4 interaction was recapitulated through co-immunopreciptation. In 3xFLAG-TCF7L1 mESC, TCF7L1 was immunoprecipitated with Dynabeads-coupled to abFLAG. Upon successful TCF7L1 enrichment, SALL4 was co-immunopreciptated and appeared as a band of approximately 165kD in western blots. Non-specific probing using normal mouse IgG coupled to Dynabeads failed to

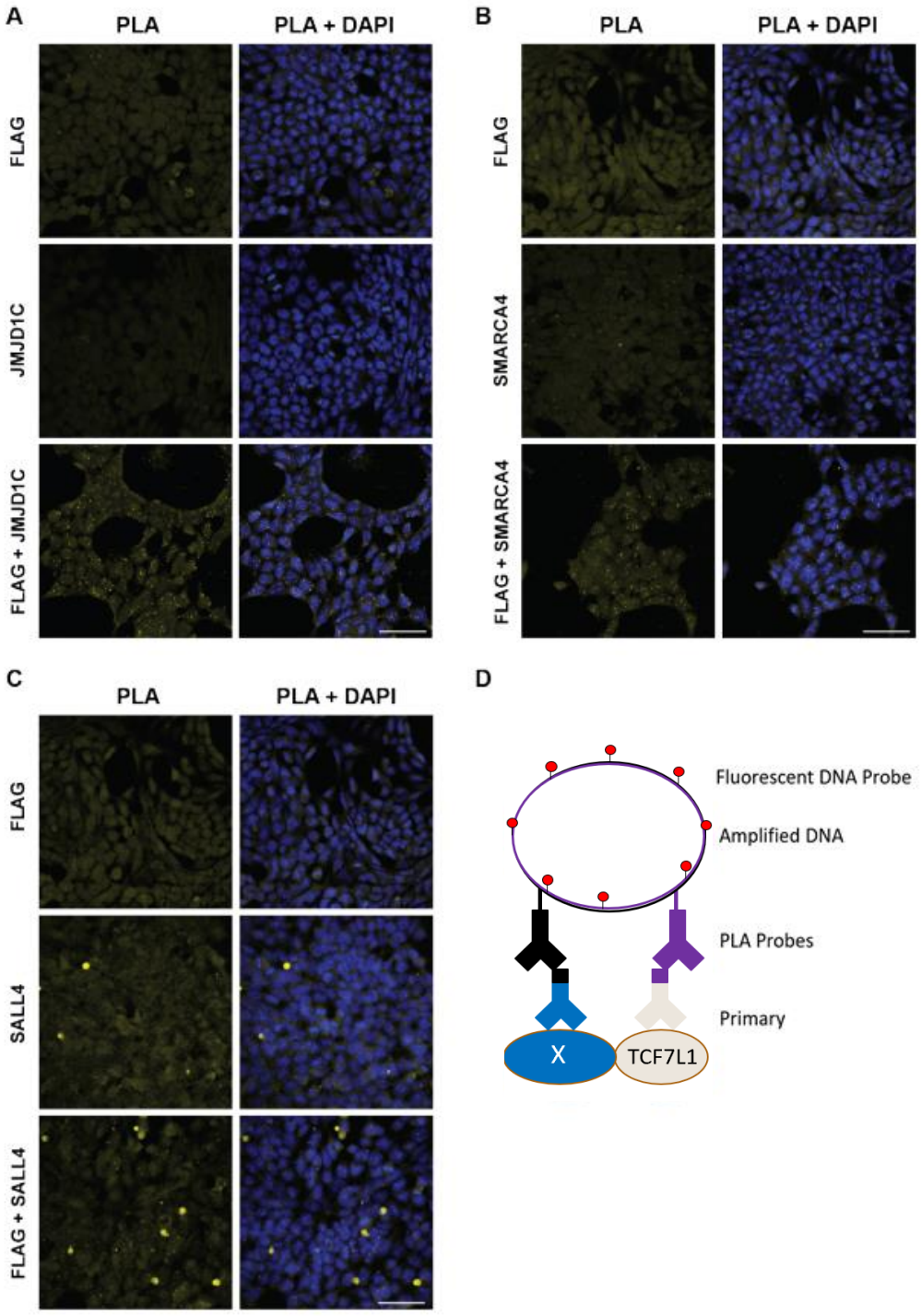

Figure 4. Proximity Ligation Assay Immunofluorescence captures TCF7L1 interactions with JMJD1C(A), SMARCA4(B) and SALL4(C).
A general schematic of the PLA architecture, depicting Protein interaction, Primary antibodies, Secondary-PLA probes, rolling circle amplified DNA, and interaction capturing Fluorescent DNA probes.

enrich TCF7L1 and SALL4 as shown in Figure 5.

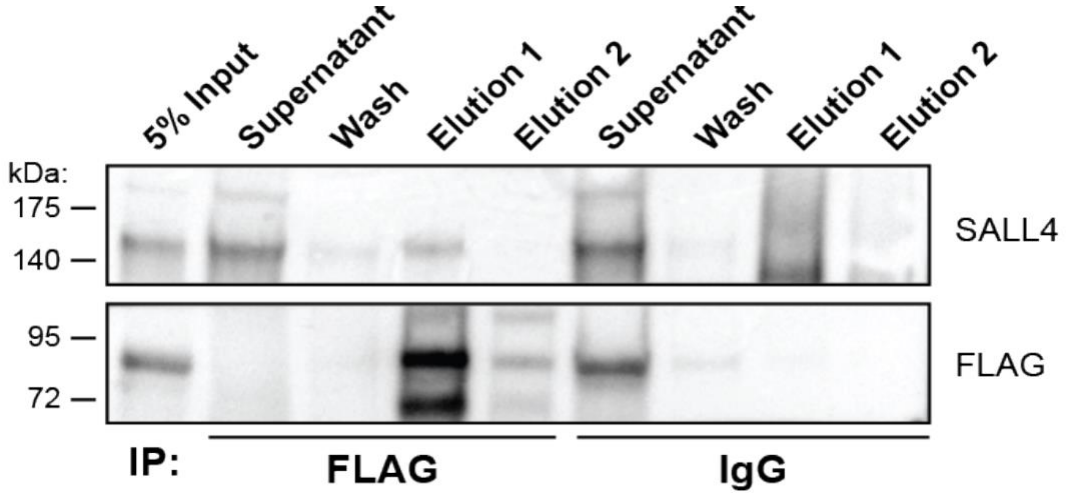

Figure 5. Co-IP validation of the TCF7L1-SALL4 interaction.
Successful enrichment of TCF7L1 by using anti-FLAG antibody immunoprecipitation co-elutes SALL4. Negative control-normal mouse IgG is unsuccessful in enriching TCF7L1, consequently, SALL4 is absent in the elution fraction.

3.3 TCF7L1 interacts with SALL4 independent of β-catenin

As TCF7L1 and SALL4 share a common protein binding partner, β-catenin, we tested whether the TCF7L1-SALL4 interaction requires β-catenin. A TCF/LEF quadruple knockout mESC cell line (QKO) was previously generated by our lab and lacks expression of all 4 TCF/LEF family members. Also generated by our lab, the TCF/LEF β-catenin (TLB) knockout cell line lacks β-catenin in addition to all TCF/LEFs. The TCF7L1 and SALL4 interaction was tested by transiently transfecting a TCF7L1-3xFLAG overexpression construct into QKO and TLB mESCs. Interestingly, immunoprecipitating the transiently transfected TCF7L1-3xFLAG from TLB mESC lysates did not abolish the SALL4 interaction (Figure 6). This indicates that although β-catenin is a common binding partner for both proteins, it is not part of the same complex, or it does not play a major role

in bridging the TCF7L1-SALL4 interaction. This suggests that the TCF7L1-SALL4 interaction is most likely β-catenin-independent in WT cells.

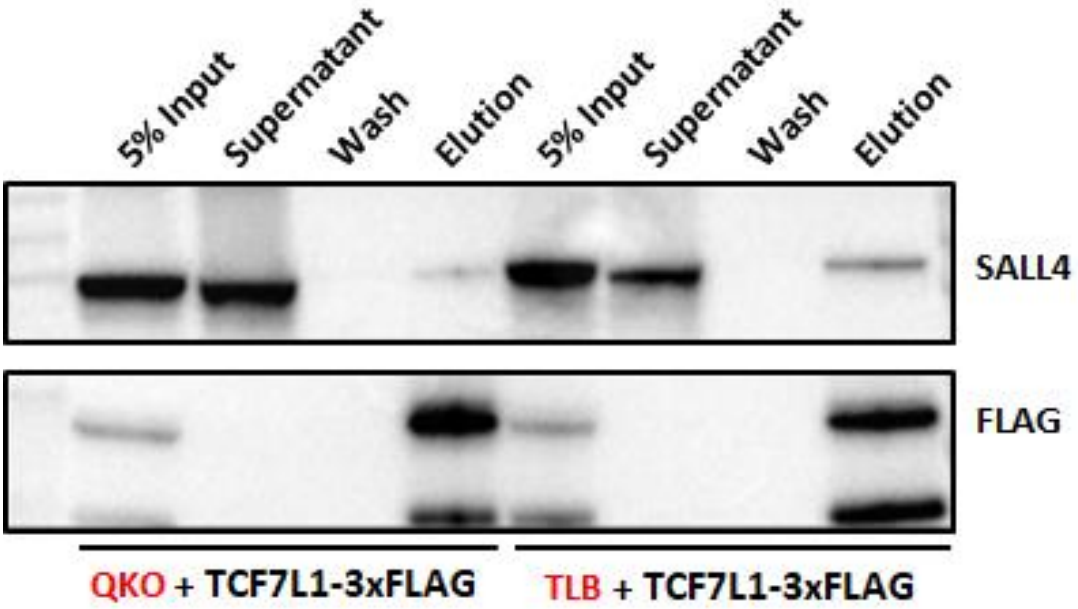

Figure 6. TCF7L1 interacts with SALL4 in the absence of β-catenin.
Successful enrichment of transiently transfected TCF7L1-3xFLAG in QKO and TLB mESCs by immunoprecipitation resulted in co-immunoprecipitation of SALL4 in both cell lines.

3.4 The TCF7L1-SALL4 and TCF7-SALL4 Interaction requires DNA.

As TCF7L1 and SALL4 are DNA binding proteins, we investigated whether TCF7L1 interacts with SALL4 through a DNA bridge. To test this, we treated cell lysates with 50 units of Benzonase to completely digest both naked and protein-bound DNA. Notably, Benzonase treatment rendered a TCF7L1-SALL4 interaction undetectable by co-IP (Figure 7A). To test whether TCF7L1 or TCF7 are bound on the same region of the DNA as SALL4, we modified the previous experiment by substituting Benzonase with DNaseI, that can only digest naked DNA. As shown in Figure B, 5U DNaseI treatment diminished the amount of

co-eluted SALL4, suggesting that the TCF7L1 interacts with SALL4 through different loci of the DNA.

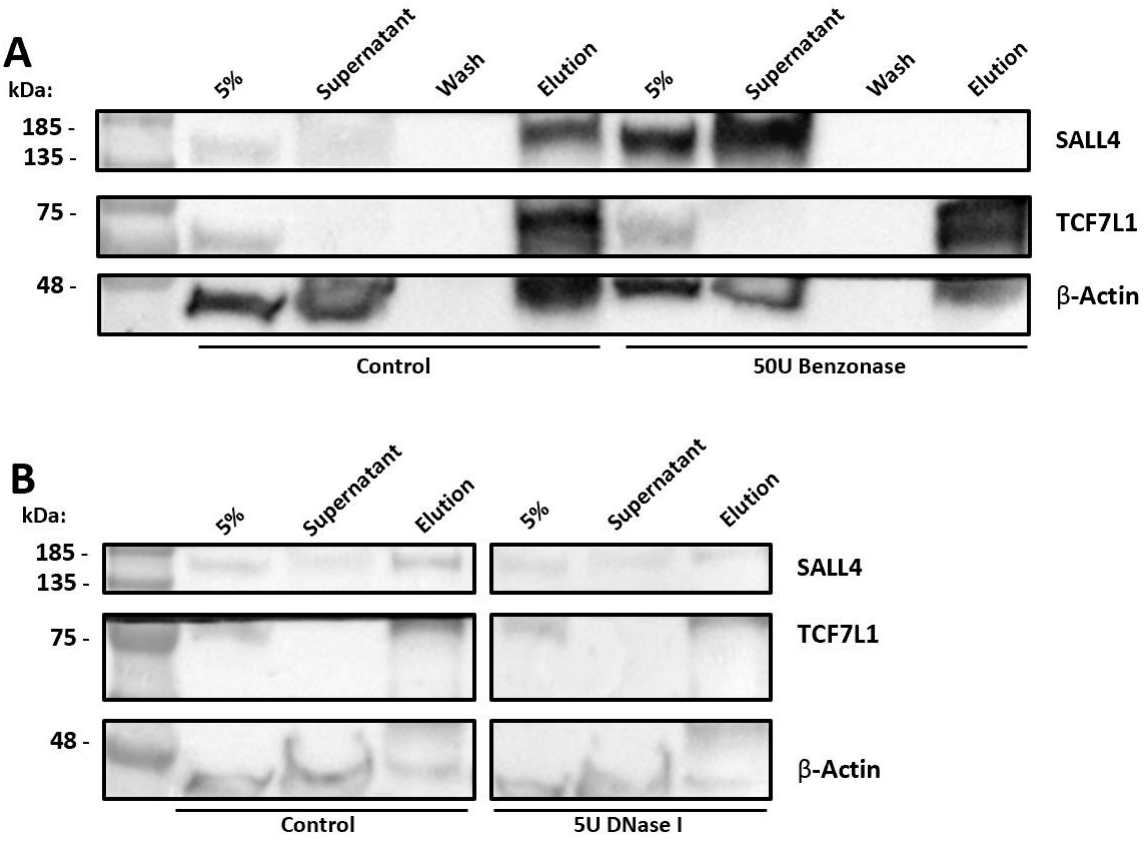

Figure 7. DNA Digestion with Benzonase and DNase I disrupt the TCF7L1-SALL4 interaction.

3.5 SALL4 Mimics Wnt Signaling Activation

The Wnt-reporter TOP-FLASH quantitatively measures Wnt activity via a luciferase reporter under the control of WRE-TCF/LEF binding sites. As shown in Figure 8, overexpressing SALL4 in DMSO-treated cells modestly increases Wnt reporter activity, mimicking Wnt activation. SALL4, as a downstream Wnt signaling target, may play a role in aiding the activation of target genes that may require SALL4 cooperativity. Interestingly, overexpressing SALL4 in Wnt-activated conditions decreased reporter activity, suggesting

a SALL4 negative feedback mechanism that may fine tune or regulate Wnt target gene activation.

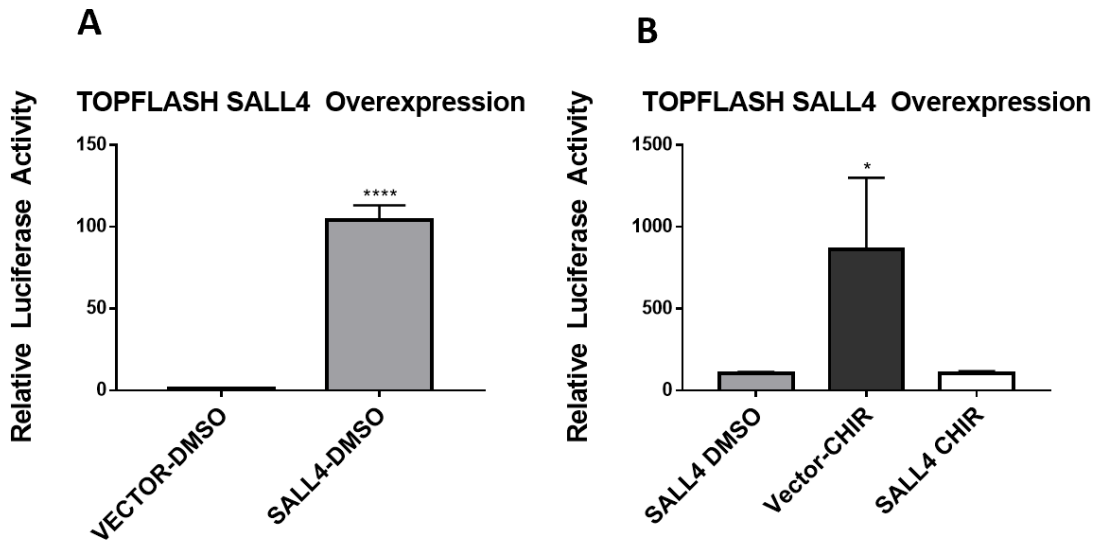

Figure 8. TOP-FLASH Reporter Assay in mESCs transiently transfected with an empty vector or a SALL4 overexpression vector.
Compared to the empty vector, Sall4 overexpression increased Wnt target response in DMSO conditions(A). In CHIR99021 conditions, overexpressing SALL4 downregulated Wnt reporter activity (B). Graph A: Vector DMSO plot n = 3, SALL4-DMSO plot n = 3, Unpaired t-test, $p < 0.0001$. Graph B: Vector-CHIR plot n = 3, SALL4 CHIR plot n = 3, One-way ANOVA, $p<0.04$.

3.6 TCF7L1 directly downregulates Tbx3

Given SALL4's known pluripotency promoting functions, we examined the literature for essential pluripotency genes that may be regulated by TCF7L1 and vice versa. Published literature reported direct binding of TCF7L1 to the promoter of Tbx3 as determined through ChIP-qPCR. To elucidate TCF7L1's mode of Tbx3 regulation, TCF7L1 expression was induced in a TetON-TCF7L1-3xFLAG mESC cell line. 24 hours post induction with 1 µg/mL doxycycline, TCF7L1 mRNA and protein levels increased

approximately 6-fold (Figure 9). Notably, Tbx3 levels decreased 2-fold concomitant with the increase of its validated repressed-downstream target, Dppa3.

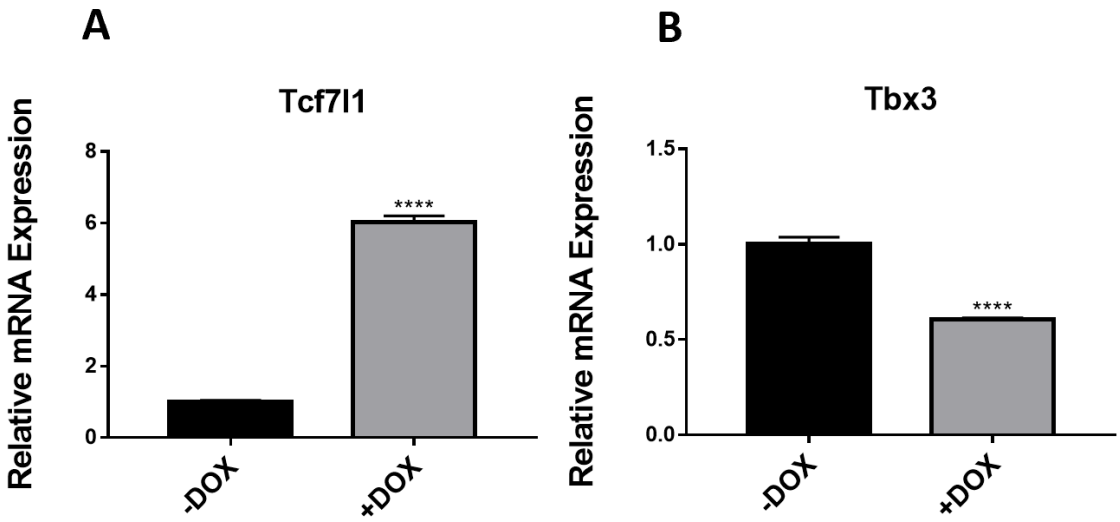

Figure 9. Doxycycline-induced overexpression of TCF7L1 downregulates Tbx3.
Addition of 1 µg/mL Doxycycline to TetON-TCF7L1-3xFLAG mESC downregulates Tbx3. Graph A: TCF7L1 -Dox plot n = 3, TCF7L1 +Dox plot n = 3, Unpaired t-test, $p<0.0001$. Graph B: Tbx3 -Dox plot n = 3, Tbx3 +Dox plot n = 3, Unpaired t-test, $p<0.0001$.

3.7 Stable Transfection of pCMV-SALL4-3xFLAG into E14-mESC

As illustrated in Figure 10. western blotting validated the stable overexpression of SALL4-3xFLAG in clones C.8, C.9, C.10, and C.11 by FLAG antigen probing.

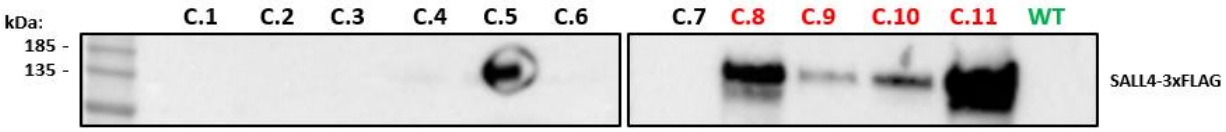

Figure 10. Western Blot analysis of selected mESC colonies stably transfected with pCMV-SALL4-3xFLAG.
mESC-E14TG2A was transfected by using pCMV-SALL4-3xFLAG and pCAG-Puro. Among 11 colonies screened after 48-hour puromycin selection C.8, C.9, C.10, and C.11, were true colonies, validated through the FLAG epitope tag.

3.8 Tbx3 is upregulated in TCF7L1 nulls and Sall4-overexpresing mESCs

Previously, we showed that *Tbx3* is a repressed target of TCF7L1. Here we investigated the mRNA transcripts of *Wnt3a, Tbx3,* and a Tbx3 downstream repressed target-*Dppa3*. As expected, *Tbx3* mRNA transcripts increased approximately 6-fold upon knocking out *Tcf7l1*, along with a decrease in *Dppa3* transcripts. Interestingly, mESCs stably overexpressing SALL4 similarly altered the transcript levels of *Tbx3, Dppa3,* and *Wnt3a* as observed in Tcf7l1 knockout mESCs (Figure 11).

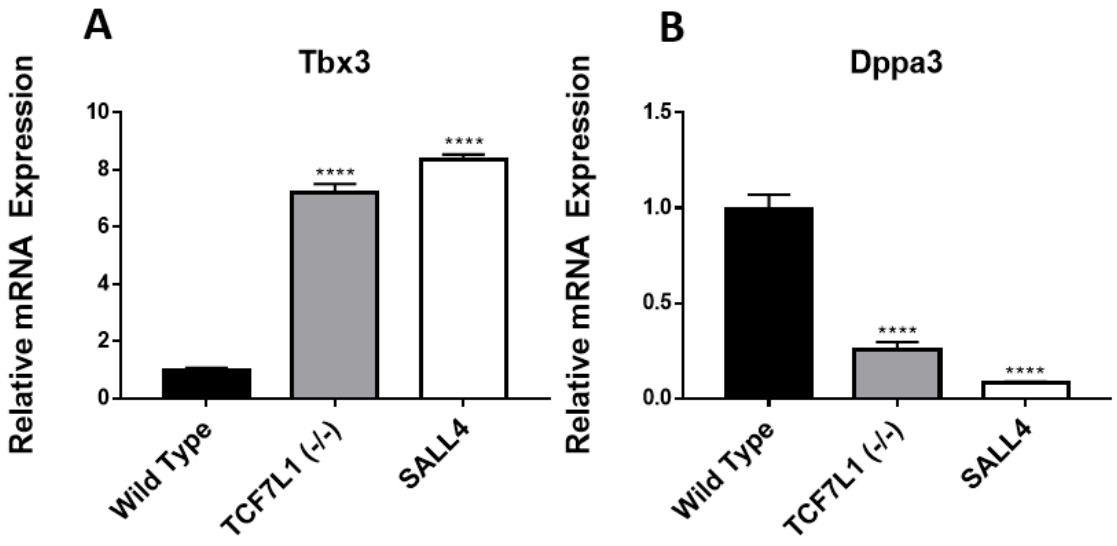

Figure 11. TCF7L1-knockout and Sall4-overexpression upregulate *Tbx3* and downregulates known Tbx3-repressive target, *Dppa3*.
Graph A: Tbx3-Wild Type plot n = 4, Tbx3-TCF7L1 (-/-) plot n=4, Tbx3-SALL4 plot n=4, One-way ANOVA, $p<0.001$. Graph B: Dppa3-Wild Type plot n = 4, Dppa3-TCF7L1 (-/-) plot n=4, Dppa3-SALL4 plot n=4, One way-ANOVA, $p<0.001$.

3.9 TCF7 also interacts with SALL4

As TCF7L1 shares structural homology and binding sites with other members of the TCF/LEF family, we wanted to test whether other TCF/LEFs can also bind SALL4. As the second most abundant member of the TCF/LEFs in mESCs, we pursued further Co-IP interaction studies in E14TG2A-mESCs with 3xFLAG knocked into the endogenous locus of *TCF7*. Following the protocol used for TCF7L1, successfully enriched FLAG-tagged

TCF7 co-eluted SALL4, detected through immunoblotting (Figure 12). This confirmed our hypothesis that TCF7 also interacts with SALL4. As SALL4 bound both TCF7 and TCF7L1, we wanted to test whether SALL4 may play a role in a proposed β-catenin-mediated TCF/LEF switch mechanism. To test this, we activated Wnt signaling with the GSK3 inhibitor, CHIR99021, to see if the TCF7-SALL4 interaction is altered upon nuclear accumulation of β-catenin. TCF7 bound to SALL4 as determined through Co-IP. However, compared to TCF7L1-SALL4 Co-IPs, less SALL4 was co-eluted with TCF7 in control conditions (DMSO). Furthermore, in CHIR99021 conditions, we observed more co-eluted SALL4 with TCF7 Co-IPs (Figure 12).

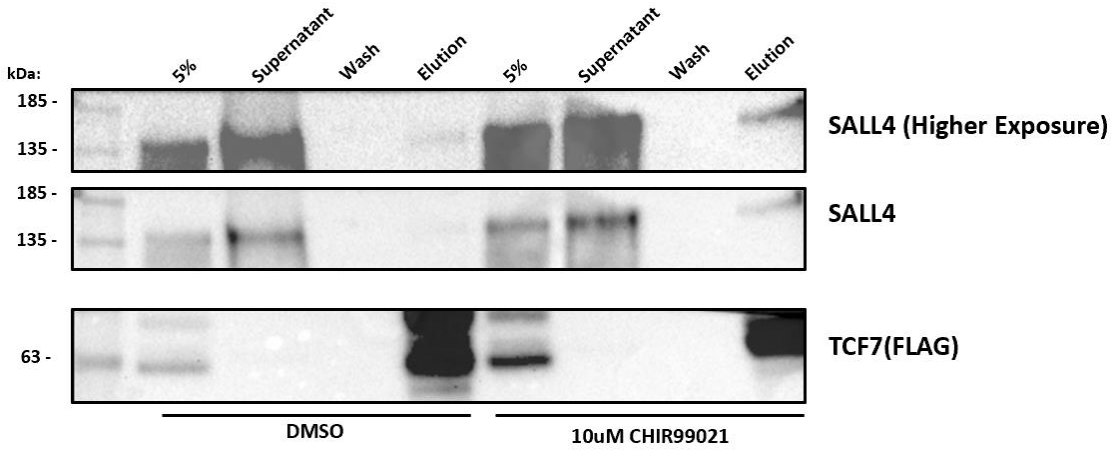

Figure 12. TCF7 interacts with SALL4 in DMSO/CHIR99021 conditions.
Enrichment of TCF7-3xFLAG co-eluted SALL4 in both DMSO and CHIR99021 conditions. More SALL4 was co-eluted in CHIR99021 conditions.

3.10 Successful IPTG induction of SALL4 protein expression in bacteria

Post IPTG induction, SALL4 protein was most highly expressed at the 3-hour time point in Rosetta (DE3) competent cells as indicated with the red arrow in Figure 13. Unfortunately, we were unable to express TCF7L1 in BL21 or Rosetta (DE3) competent cells. Further optimization is necessary.

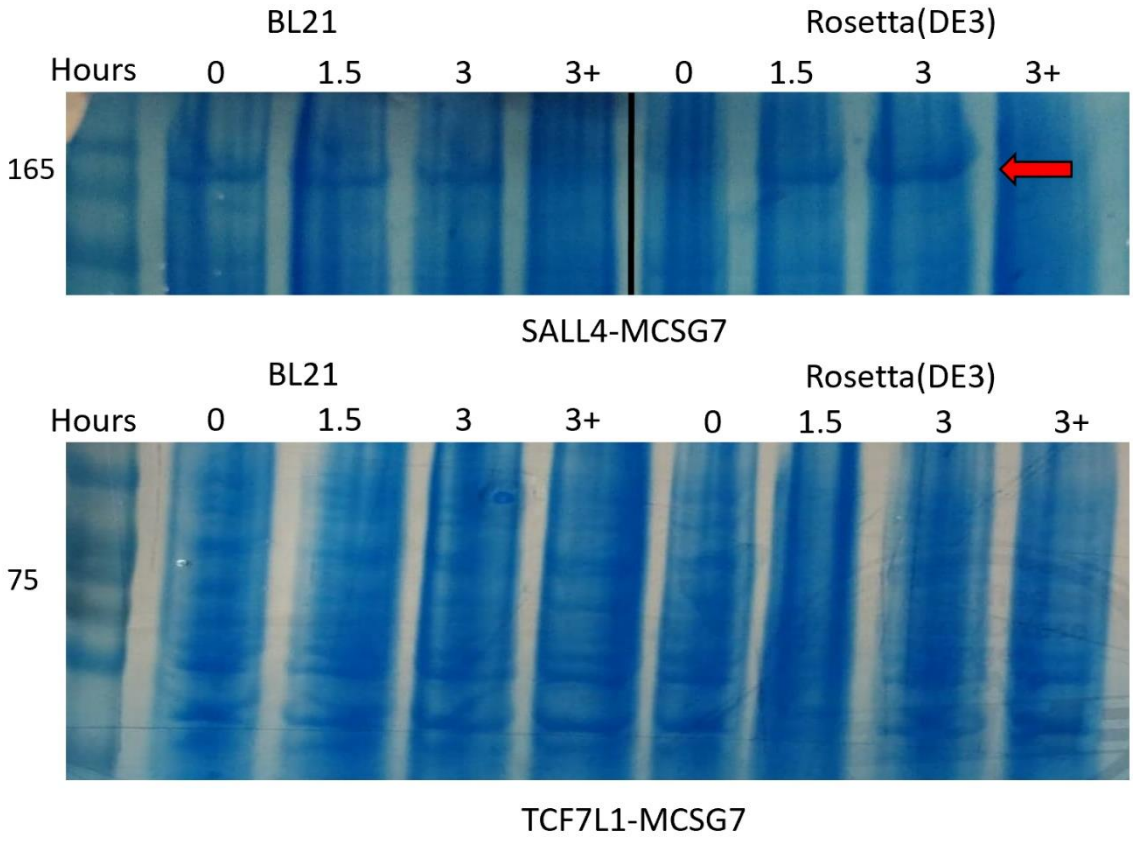

Figure 13. 1M IPTG Induction of BL21 and Rosetta(DE3) Lysogen transformed with MCSG7-SALL4 and MCSG7-TCF71.
Red arrow indicates the expression SALL4 protein at the 3 hour time point in Rosetta (DE3) competent *E.coli* cells.

CHAPTER 4: DISCUSSION

4.1 Summary of Findings

To better understand stem cell biology via Wnt signaling regulation, TCF7L1 and its potential binding partners were interrogated. From previous efforts in our lab, TCF7L1-interacting protein candidates were obtained by using the BioID assay, which employed biotinylation of TCF7L1-proximal proteins for selective isolation and identification. Categorized based on gene ontology using Database for Annotation, Visualization and Integrated Discovery (DAVID), proteins related to Wnt signaling, PcG complex, Nuclear receptors, BAF complex, Spalt-like, MLL and more were identified. This alluded to the complexity of TCF7L1 proteomics that requires elucidation (Figure 14).

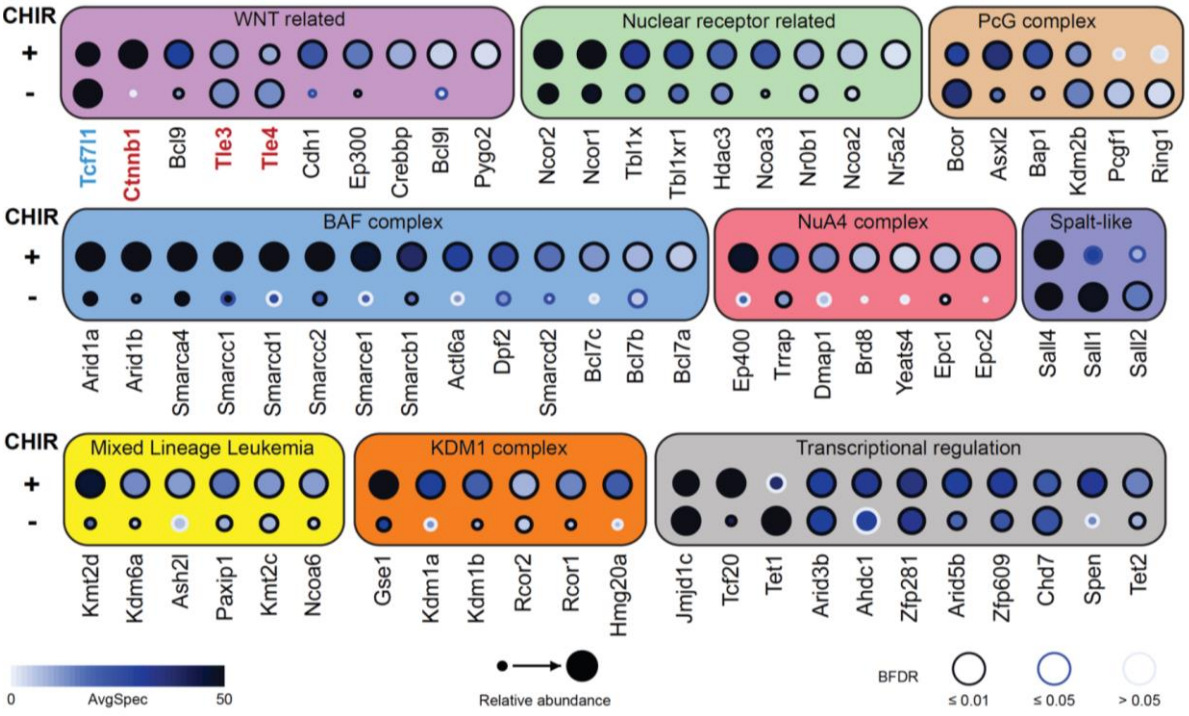

Figure 14. Putative TCF7L1 interacting proteins identified through BioID in mESCs treated with DMSO/10 µM CHIR99021.
Biotin ligase tagged TCF7L1 biotinylated proximal proteins and allowed for their isolation/identification. Proteins were categorized based on gene ontology using DAVID. Statistical analysis was implemented by using the Bayesian False Discovery Rate (BFDR).

As positive controls, well known interactors of TCF7L1 including β-catenin were isolated and identified through mass spectrometric analysis of TCF7L1 BioID samples.

PLA is a proximity fluorescence-based technique that detects PPIs based on the addition of two specific primary antibodies probing for individual proteins that are being interrogated as interactors. PPIs were revealed as punctae upon specific combinations of primary antibodies that probed for FLAG-JMJD1C, FLAG-SMARCA4, and FLAG-SALL4 in mESCs with a 3xFLAG knocked into the endogenous locus of TCF7L1.

In agreement with previously reported TCF7L1 localization studies, the majority of the punctae were observed in nuclei (Sierra et al., 2018), suggesting that interactions were localized to the nucleus. As TCF7L1, JMJD1C, and SMARCA4 are predicted or known to exclusively localize in the nucleus it makes sense that the interaction-revealing punctae are enriched within the nucleus (Dudek, Pfaff, & Schwemmle, 2016; Sáez et al., 2016). However, SALL4 has been reported to localize to both the cytoplasm and the nucleus, but we only observed its interaction with TCF7L1 in the nucleus (Yue et al., 2015). This suggests that, in mESCs, TCF7L1 is a nucleus exclusive protein and the TCF7L1 and SALL4 interaction most likely involves the regulation of target genes, given both proteins' propensity for DNA binding

Among the four protein interactions validated with PLA, SALL4 was further validated to interact with TCF7L1 by co-immunoprecipitation. Previous attempts to validate TCF7L1 interactions with JMJD1C, and SMARCA4 through co-immunoprecipitation were unsuccessful.

One of the biggest challenges of co-immunoprecipitation is maintaining the structural integrity of the proteins in study post lysis, to maintain the PPI. Given the large protein size

of JMJD1C (260kD), and SMARCA4 (185kD), the proteins were highly unstable in lysis buffer conditions, illustrated by protein degradation smears observed through immunoblotting. The unsuccessful Co-IPs may be due to inherent transient/weak nature of the PPI, sensitivity to salt conditions, or the requirement/absence of $MgCl_2$ and DTT. To overcome this issue, the use of a reversable crosslinker such as dithiobis(succinimidyl propionate)) (DSP) may help to preserve the interactions, although it may introduce elevated background false-positive interactions.

SALL4, the smallest among the three proteins validated through PLA, has been reported to interact with β-catenin (Ma Y et al., 2006). Successfully immunoprecipitating SALL4-3xFLAG, co-eluted a significant amount of β-catenin, suggesting a strong or frequent interaction. β-catenin, as a prominent interactor of all TCF/LEF family members, led us to believe that the TCF7L1-SALL4 interaction could be mediated by β-catenin. To test this, co-IP of TCF7L1and SALL4 was repeated in β-catenin knockout E14 mESCs. Interestingly, TCF7L1 and SALL4 maintained their interaction in the absence of β-catenin, as shown on Figure 6, indicating that the interaction does not require β-catenin as a potential bridging protein.

β-catenin has a molecular mass of 90 kDa, which is most likely too large to passively cross the nuclear pores without assistant proteins. β-catenin lacks prototypical nuclear localization (NLS) and a nuclear export sequences (NES) that are essential to enter and exit the nucleus via import/exportin systems, yet it has been shown to efficiently cross the nuclear membrane (Eleftheriou, Yoshida, & Henderson, 2001; Wiechens & Fagotto, 2001). SALL4 overexpression in both the nucleus and cytoplasm have their own unique clinical outcomes as reported in (Yue et al., 2015) , suggesting that SALL4 plays an important role

in cellular homeostasis in both the cytoplasm and the nucleus (Yue et al., 2015). Not surprisingly, at least one canonical NLS has been identified in SALL4. Given the strong propensity of SALL4 to bind β-catenin it may be possible that β-catenin enters and exits the nucleus through a "piggyback" relationship with SALL4, with no functional relevance to the TCF7L1-SALL4 interaction.

As a member of the TCF/LEF family of transcription factors, TCF7L1 is well characterized as a DNA binding transcription factor through its HMG domain, and it regulates expression of multiple gene targets (Giese et al., 1995). Through its zinc finger motif, SALL4 also binds DNA and regulates gene expression though the recruitment of epigenetic complexes (Yang, 2018). Based on the DNA-binding nature of TCF7L1 and SALL4, we postulated that the TCF7L1-SALL4 interaction may play a role in gene regulation and that they were held together by the DNA element they bind.

To test this, we enzymatically degraded DNA in cell lysates by using Benzonase prior to protein isolation and centrifugation. As shown in figure 7A, addition of 50U of Benzonase increased the amount of SALL4 in 15 µg of protein lysate input compared to control lysates. SALL4 functions to repress gene targets through the recruitment of epigenetic complexes (Yang, 2018). Therefore, liberating SALL4 from condensed inactive chromatin via Benzonase most likely increased its solubility and recovery.

The TCF7L1-SALL4 interaction was abolished upon Benzonase treatment. Refining our finding, we tested whether TCF7L1 and SALL4 occupied the same region of the DNA. As it only digests naked DNA, DNase I was utilized to further interrogate the TCF7L1-SALL4-DNA complex. DNase I-treated lysates eluted less SALL4 in TCF7L1 co-IPs, suggesting that a stretch of naked DNA exists between the SALL4-TCF7L1 complex.

Furthermore, we have demonstrated that SALL4 is capable of activating a luciferase-based Wnt reporter. SALL4, as a downstream Wnt target gene, may act as a positive feedback regulator of certain target genes. TCF7L1-β-catenin interactions have been reported to be a requirement for Wnt target activation, despite the predominant role of TCF7L1 as a repressor. It has been reported that TCF7L1-β-catenin mediated gene activation can occur indirectly through derepression of LEF1 (Wu et al., 2012). In this case, derepression may occur not through β-catenin, but SALL4.

It is interesting to observe the interaction between two factors that promote opposite states of pluripotency/differentiation. The interaction of a pro-pluripotency protein (SALL4), and a pro-differentiation protein (TCF7L1) prompted us to hypothesize an antagonistic relationship between SALL4 and TCF7L1. Therefore, we looked in the literature for pluripotency essential gene targets regulated by SALL4 and TCF7L1. As TCF/LEFs have preferential binding to their respective HMG-TCF/LEF binding domains, we narrowed the search for TCF7L1 regulated gene targets.

TCF7L1 has been shown to bind the promoter of *Tbx3* through ChIP-qPCR (Han et al., 2010). *Tbx3* is a downstream Wnt target gene known to regulate the expression of key embryonic stem cell factors (Han et al., 2010). In addition to maintaining pluripotency, Tbx3 is heavily involved in developmental processes covering limb, apocrine gland, and genital development (Koboldt et al., 2012). Illustrated in Figure 9, conditionally overexpressing TCF7L1 decreased the mRNA transcript of *Tbx3*, suggesting that TCF7L1 is repressing *Tbx3* transcription. Knocking out *Tcf7l1* upregulated *Tbx3*.

Interestingly, overexpressing SALL4 was also able to upregulate *Tbx3*, suggesting that SALL4 may play a role in the suppression of TCF7L1 to overcome the repressive barrier

placed on *Tbx3* (Figure 11). Mechanistically, this may be a result of TCF7L1 co-repressor dislodgement by SALL4, as both proteins are able to bind the co-repressor HDAC1. The dislodgement of HDAC1 and TLE3 from TCF7L1 has been demonstrated previously through the action of another zinc finger protein, E4F1 (Ro & Dawid, 2011). Therefore, it is possible that the zinc finger protein, SALL4 may also have this capability, although future experiments will need to be conducted to validate this theory. Combining all of our findings, SALL4 may target TCF7L1, perhaps only dominant-negative isoforms lacking a β-catenin binding domain, to activate at least a subset of target genes, such as *Tbx3*. As it shares homology and structural motifs with TCF7L1, we tested whether TCF7 can also bind SALL4. We were able to co-elute SALL4 upon enrichment of TCF7-3xFLAG via immunoprecipitation, however to a lesser degree compared to TCF7L1.

Interestingly, upon Wnt activation with GSK3-inhibitor, CHIR99021, we observed an increased SALL4 co-elution in TCF7 immunoprecipitates, suggesting that β-catenin may positively mediate the interaction (Figure 12). This observation was unique to TCF7, as TCF7L1-SALL4 binding remained the same with or without CHIR99021 treatment. Alternatively, the increase in SALL4 elution with TCF7 may simply be a result of CHIR99021-induced upregulation of TCF7, as TCF7 is a known target of Wnt signaling. Observing that the TCF/LEF interaction with SALL4 is not unique to only TCF7L1, but also to TCF7 raises the potential importance of SALL4 in all TCF/LEF mediated gene regulation, at least in mESCs. As SALL4 is known to recruit epigenetic complexes to repress or activate gene targets, it is plausible to suggest that SALL4 may be involved in the TCF/LEF regulatory mechanism (Yang, 2018). Future efforts will be placed on capturing the interaction of SALL4 with additional TCF/LEFs, such as TCF7L2 and LEF1,

to bolster the theory of a SALL4-TCF/LEF role in Wnt signaling in mESCs (and possibly other cell types).

To study the occupancy of the *Tbx3* promoter by TCF7L1, and potentially SALL4, we screened the *Tbx3* promoter sequence for TCF/LEF-HMG binding sites using JASPAR and found 5 potential sites. We also screened for C2-H2 zinc finger binding motifs that could potentially be bound by SALL4 by using JASPAR and found many sites overlapping or located close to potential TCF/LEF binding sites. These regions were selected for ChIP-qPCR investigation of the *Tbx3* promoter. Subsequent ChIP experiments were performed using primers specific to these regions to develop a fold-enrichment baseline.

4.2 Future Directions

4.2.1 Protein-Overexpression/Purification

We have demonstrated that TCF7L1 and TCF7 interaction with SALL4 requires DNA, most likely near promoters of Wnt target genes. TCF7L1 and TCF7 are generally considered to be repressors and activators, respectively. Identifying the common interacting protein, SALL4, with two TCFs of opposing function, raises questions regarding the potential capability of SALL4 to facilitate Wnt gene regulation through structural reorganization of the TCFs. Therefore, potential structural comparisons between the TCF7L1- and TCF7-SALL4 complexes may provide insights into the difference in transcriptional regulation and help to further our understanding of a proposed TCF/LEF switch model.

The preliminary step of cloning TCF7L1 and SALL4 cDNA into the pMCSG7-overexpression/purification vector has been completed. Further efforts must be placed on cloning TCF7 into the MCSG vector and on identifying optimal expression conditions for

TCF7, prior to upscaling protein production and purification. Given the difficulty of solubilizing large proteins, it is likely that additional troubleshooting may be necessary. Currently we have available additional versions of MCSG plasmids: pMCSG9, and pMCSG10 which have solubility enhancing tags such as the maltose binding protein tag and the Glutathione S-transferase tag respectively, which may need to be utilized if the overexpressed proteins are insoluble.

4.4.2 Interrogating the Tbx3 Promoter Occupancy by TCF7L1

Tbx3, a Wnt target gene that is transcriptionally repressed and bound by TCF7L1 may also be regulated by SALL4. SALL4 overexpression promotes an increase in *Tbx3* mRNA transcripts. It would be interesting to test the validated promoter occupancy of TCF7L1 upon SALL4 overexpression, SALL4 ablation, and GSK3 inhibition. Given our findings, regarding the DNA dependency of the TCF7L1-SALL4 interaction and the antagonistic transcriptional relationship between TCF7L1 and SALL4, it is possible that TCF7L1 loses affinity to the *Tbx3* promoter upon SALL4 overexpression. To test this, future efforts must be placed in optimizing ChIP-qPCR to establish an enrichment baseline of the *Tbx3* promoter sequence by using TCF7L1 ChIP-grade antibody. To date, the mouse *Tbx3* promoter sequence was screened for potential TCF/LEF binding sites, and primers have been established. After the base level enrichment of Tbx3 promoter is established in mESCs, the TCF7L1 occupancy of the promoter can finally be interrogated in respect to Wnt signaling and SALL4.

4.2.3 Elucidating the Molecular Action of SALL4 on TCF7L1 in Wnt Signaling

If it is demonstrated that the *Tbx3* promoter occupancy of TCF7L1 does not change with the overexpression of SALL4, it may also be possible that SALL4 simply binds DNA near

TCF7L1 to promote the dislodgment of essential co-repressors. Efforts have been made to Co-IP TLE3 in 3x-FLAG TCF7L1 mESCs by using anti-FLAG antibodies. Unfortunately, we had minimal success. An alternative may be to utilize PLA to initially capture the TCF7L1-TLE3 interaction. An interesting experiment to pursue is to test for the dislodgement of TLE3 from TCF7L1 by observing loss of punctae upon overexpression of SALL4 in both DMSO and CHIR99021 conditions. Referring back to our previous Wnt-reporter assay, if the TCF7L1-TLE3 interaction is abolished in SALL4 overexpression/DMSO conditions, but re-established in the SALL4/CHIR99021 condition, we will be closer to elucidating a mechanism for potential SALL4-mediated regulation of TCF7L1 function.

Conclusion

Mammalian cells are highly complex, governed by tightly regulated gene expression and protein function. Here, we described protein-level interplay of SALL4 with Wnt signaling. We revealed that SALL4 is more than a mere gene target of Wnt signaling. Through PLA, we validated that TCF7L1 interacts with JMJD1C, SMARCA4, and SALL4. We further validated the TCF7L1-SALL4 interaction through Co-IP and demonstrated that the interaction requires DNA but not β-catenin. Through a Wnt-reporter assay, SALL4 involvement in Wnt signaling output was interrogated. SALL4 is capable of activating Wnt target genes in basal conditions, however, it seems to oppositely downregulate Wnt output in highly Wnt-activated conditions. Given that TCF7L1 and SALL4 are transcription factors, we postulated that TCF7L1 and SALL4 co-regulate gene targets. Overexpressing SALL4 or knocking out TCF7L1 upregulated mRNA transcript levels of *Tbx3*, suggesting

a SALL4-mediated suppression of TCF7L1. Collectively, SALL4 may bind the *Tbx3* promoter in close proximity to TCF7L1 to inactivate TCF7L1-mediated target gene repression and promote Tbx3 expression.

References

Atcha, F. A., Syed, A., Wu, B., Hoverter, N. P., Yokoyama, N. N., Ting, J.-H. T., … Waterman, M. L. (2007). A Unique DNA Binding Domain Converts T-Cell Factors into Strong Wnt Effectors. *Molecular and Cellular Biology*, *27*(23), 8352–8363. https://doi.org/10.1128/MCB.02132-06

Balemans, W., Patel, N., Ebeling, M., Hul, E. Van, Wuyts, W., Lacza, C., … Hul, W. Van. (2002). Identification of a 52 kb deletion downstream of the. *Journal of Medical Genetics*, *39*, 91–97.

Becker, K., Ghule, P., & Stein, G. (2006). Self-Renewal of Human Embryonic Stem Cells is Supported by a Shortened G1 Cell Cycle Phase. *Journal of Cellular Physiology*, *209*(1), 883–893. https://doi.org/10.1002/JCP

Boeuf, H., Hauss, C., De Graeve, F., Baran, N., & Kedinger, C. (1997). Leukemia inhibitory factor-dependent transcriptional activation in embryonic stem cells. *Journal of Cell Biology*, *138*(6), 1207–1217. https://doi.org/10.1083/jcb.138.6.1207

Brivanlou, A., & Rossant, J. (2003). Setting Standards for Human Embryonic Stem Cells. *Stem Cell Reports*, *300*(5621), 913–916.

Brunkow, M. E., Gardner, J. C., Ness, J. Van, Paeper, B. W., Kovacevich, B. R., Proll, S., … Mulligan, J. T. (2001). Bone Dysplasia Sclerosteosis Results from Loss of the SOST Gene Product, a Novel Cystine Knot–Containing Protein. *American Journal of Human Genetics*, *68*, 577–589.

Cadigan, K. M. (2012). TCFs and Wnt/β-catenin signaling: more than one way to throw the switch. *Developmental Biology*, *98*, 1–34.

Cadigan, K. M., & Waterman, M. L. (2012). TCF / LEFs and Wnt Signaling in the Nucleus, 1–22.

Chodaparambil, J. V., Pate, K. T., Hepler, M. R. D., Tsai, B. P., Muthurajan, U. M., Luger, K., … Weis, W. I. (2014). Molecular functions of the TLE tetramerization domain in Wnt target gene repression. *EMBO Journal*, *33*(7), 719–731. https://doi.org/10.1002/embj.201387188

Cotsarelis, G., Sun, T. T., & Lavker, R. M. (1990). Label-retaining cells reside in the bulge area of pilosebaceous unit: Implications for follicular stem cells, hair cycle, and skin carcinogenesis. *Cell*, *61*(7), 1329–1337. https://doi.org/10.1016/0092-8674(90)90696-C

Cui, Y. Niziolek, P. MacDonald, B. (2011). Lrp5 functions in bone to regulate bone mass. *Nature Medicine*, *17*(6), 684–691. https://doi.org/10.1016/j.physbeh.2017.03.040

D, X., Tang, W., & Y, Y. (2016). Structure and function of the AAA+ ATPase p97/Cdc48p. *Epub*, *583*(1), 64–77. https://doi.org/10.1097/CCM.0b013e31823da96d.Hydrogen

Daniels, D. L., & Weis, W. I. (2005). β-catenin directly displaces Groucho/TLE repressors from Tcf/Lef in Wnt-mediated transcription activation. *Nature Structural and Molecular Biology*, *12*(4), 364–371. https://doi.org/10.1038/nsmb912

Dudek, A., Pfaff, F., & Schwemmle, M. (2016). Partial Inactivation of the Chromatin Remodelers SMARCA2 and SMARCA4 in Virus-Infected Cells by Caspase-Mediated Cleavage. *Journal of Virology*, *92*(16), 1–14.

Eleftheriou, A., Yoshida, M., & Henderson, B. R. (2001). Nuclear Export of Human □ -Catenin Can Occur Independent of CRM1 and the Adenomatous Polyposis Coli Tumor Suppressor *. *Journal of Biological Chemistry*, *276*(28), 25883–25888. https://doi.org/10.1074/jbc.M102656200

F., L., O., V. den B., & S., H. (2005). Distinct roles for Xenopus Tcf/Lef genes in mediating specific responses to Wnt/beta-catenin signalling in mesoderm development. *Development*, *132*(24), 5375–5385. https://doi.org/10.1242/dev.146589

Flack, J. E., Mieszczanek, J., Novcic, N., & Bienz, M. (2017). Wnt-Dependent Inactivation of the Groucho/TLE Co-repressor by the HECT E3 Ubiquitin Ligase Hyd/UBR5. *Molecular Cell*, *67*(2), 181-193.e5. https://doi.org/10.1016/j.molcel.2017.06.009

Genikhovich, G., & Technau, U. (2017). On the evolution of bilaterality. *Development*, 3392–3404. https://doi.org/10.1242/dev.141507

Giese, K., Kingsley, C., Kirshner, J. R., & Grosschedl, R. (1995). Assembly and function of a TCRα enhancer complex is dependent on LEF-1-induced DNA bending and multiple protein-protein interactions. *Genes and Development*, *9*(8), 995–1008. https://doi.org/10.1101/gad.9.8.995

Glorieux, F. H., Devogelaer, J. P., Durigova, M., Goemaere, S., Hemsley, S., Jakob, F., … Winkle, P. J. (2017). BPS804 Anti-Sclerostin Antibody in Adults With Moderate Osteogenesis Imperfecta: Results of a Randomized Phase 2a Trial. *Journal of Bone and Mineral Research*, *32*(7), 1496–1504. https://doi.org/10.1002/jbmr.3143

Gong, Y., Allgrove, J., van den Boogaard, M. J., Baron, R., Steinmann, B., Fukai, N., … Wang, H. (2001). LDL receptor-related protein 5 (LRP5) affects bone accrual and eye development. *Cell*, *107*(4), 513–523. Retrieved from http://www.ncbi.nlm.nih.gov/pubmed/11719191%5Cnhttp://www.ncbi.nlm.nih.gov/pubmed/11719191?ordinalpos=29&itool=EntrezSystem2.PEntrez.Pubmed.Pubmed_ResultsPanel.Pubmed_DefaultReportPanel.Pubmed_RVDocSum

Gottardi, C. J., & Peifer, M. (2008). Terminal Regions of β-Catenin Come into View. *Structure*, *16*(3), 336–338. https://doi.org/10.1016/j.str.2008.02.005

Green, D., Whitener, A. E., Mohanty, S., & Lekven, A. C. (2015). Vertebrate Nervous System Posteriorization : Grading the Function of Wnt Signaling. *Developmental Dynamics*, 507–512. https://doi.org/10.1002/DVDY.24230

Gris, D. (2008). Activation of Wingless targets requires bipartite recognition of DNA by TCF. *Current Biology*, *18*(23), 1877–1881. https://doi.org/10.1038/mp.2011.182.doi

Hadjantonakis, A. K., MacMaster, S., & Nagy, A. (2002). Embryonic stem cells and mice expressing different GFP variants for multiple non-invasive reporter usage within a single animal. *BMC Biotechnology*, *2*, 1–9. https://doi.org/10.1186/1472-6750-2-11

Han, J., Yuan, P., Yang, H., Zhang, J., Soh, B. S., Li, P., … Lim, B. (2010). Tbx3 improves the germ-line competency of induced pluripotent stem cells. *Nature*, *463*(7284), 1096–1100. https://doi.org/10.1038/nature08735

He, X. (2004). LDL receptor-related proteins 5 and 6 in Wnt/ -catenin signaling: Arrows point the way. *Development*, *131*(8), 1663–1677. https://doi.org/10.1242/dev.01117

Kabiri, Z., Greicius, G., Madan, B., Biechele, S., Zhong, Z., Zaribafzadeh, H., … Virshup, D. M. (2014). Stroma provides an intestinal stem cell niche in the absence of epithelial Wnts. *Development*, *141*(11), 2206–2215. https://doi.org/10.1242/dev.104976

Keller, G. M. (1995). In vitro differentation of embryonic stem cells. *Current Opnion InCell Biology*, *7*(6), 862–869.

Kim, C.-H., Oda, T., Itoh, M., & Chitnis, A. (2000). Repressor activity of Headless/Tcf3 is essential for vertebrate head formation. *Nature*, *407*(6806), 913–916. https://doi.org/10.1038/mp.2011.182.doi

Kimelman, D., & Xu, W. (2006). β-Catenin destruction complex: Insights and questions from a structural perspective. *Oncogene*, *25*(57), 7482–7491. https://doi.org/10.1038/sj.onc.1210055

Koboldt, D. C., Fulton, R. S., McLellan, M. D., Schmidt, H., Kalicki-Veizer, J., McMichael, J. F., … Palchik, J. D. (2012). Comprehensive molecular portraits of human breast tumours. *Nature*, *490*(7418), 61–70. https://doi.org/10.1038/nature11412

Kramps, T., Peter, O., Brunner, E., Nellen, D., Froesch, B., Chatterjee, S., … Basler, K. (2002). Wnt/Wingless signaling requires BCL9/legless-mediated recruitment of pygopus to the nuclear β-catenin-TCF complex. *Cell*, *109*(1), 47–60. https://doi.org/10.1016/S0092-8674(02)00679-7

Kwon, G., Viotti, M., & Hadjantonakis, A.-K. (2016). The endoderm of the mouse embryo arises by dynamic widespread intercalation of embryonic and

extraembryonic lineages. *Developmental Cell*, *15*(4), 509–520. https://doi.org/10.1016/j.devcel.2008.07.017.The

Lau, W. D., Peng, W. C., Piet, G., & Clevers, H. (2014). The R-spondin/Lgr5/Rnf43 module: regulator of Wnt signal strength. *Genes & Development*, *28*(4), 305–316. https://doi.org/10.1016/0014-5793(83)80585-7

Laurie A. Boyer. (2005). Core Transcriptional Regulatory Circuitry in Human Embryonic Stem Cells. *Cell*, *122*(6), 947–956. https://doi.org/10.1016/j.cell.2005.08.020.Core

Lim, X., Tan, S. H., Yu, K. Lou, Lim, S. B. H., & Nusse, R. (2016). Axin2 marks quiescent hair follicle bulge stem cells that are maintained by autocrine Wnt/β-catenin signaling. *Proceedings of the National Academy of Sciences of the United States of America*, *113*(11), E1498-505. https://doi.org/10.1073/pnas.1601599113

Liu, C., Li, Y., Semenov, M., Han, C., Baeg, G., Tan, Y., … Signaling, C. (2002). Control of β-Catenin Phosphorylation/Degradation by a Dual-Kinase Mechanism. *Cell*, *108*, 837–847.

Loots, G. G., Kneissel, M., Keller, H., Baptist, M., Chang, J., Collette, N. M., … Rubin, E. M. (2005). Genomic deletion of a long-range bone enhancer misregulates sclerostin in Van Buchem disease. *Genome Research*, *15*(7), 928–935. https://doi.org/10.1101/gr.3437105

Lu, W. (2010). supression of Wnt/beta catenin signaling inhibits prostate cancer cell prliferation. *European Journal of Pharmacology*, *602*(1), 8–14. https://doi.org/10.1016/j.ejphar.2008.10.053.Suppression

Ma Y, Cui W, Yang J, Qu J, Di C, Amin HM, … Chai, L. (2006). SALL4, a novel oncogene, is constitutively expressed in human acute myeloid leukemia (AML) and induces AML in transgenic mice. *Blood*, *108*(8), 2726–2735. https://doi.org/10.1182/blood-2006-02-001594.Supported

Martin, G. R. (1981). Isolation of a pluripotent cell line from early mouse embryos cultured in medium conditioned by teratocarcinoma stem cells. *Proc Natl Acad Sci U S A*, *78*(12), 7634–7638. https://doi.org/10.1038/292154a0

Mascetti, V. L., & Pedersen, R. A. (2016). Contributions of Mammalian Chimeras to Pluripotent Stem Cell Research. *Cell Stem Cell*, *19*(2), 163–175. https://doi.org/10.1016/j.stem.2016.07.018

Matsuda, T., Nakamura, T., Nakao, K., Arai, T., Katsuki, M., Heike, T., & Yokota, T. (1999). STAT3 activation is sufficient to maintain an undifferentiated state of mouse embryonic stem cells. *EMBO Journal*, *18*(15), 4261–4269. https://doi.org/10.1093/emboj/18.15.4261

Mclaren, A. (2001). Ethical and social considerations of stem cell research, *414*(November), 129–131. Retrieved from www.nature.com

Moon, R. T., & Kimelman, D. (1998). From cortical rotation to organizer gene expression : toward a molecular explanation of axis specification in Xenopus. *BioEssays*, 536–545.

Moreira, S., Polena, E., Gordon, V., Abdulla, S., Mahendram, S., Cao, J., … Doble, B. W. (2017). A Single TCF Transcription Factor, Regardless of Its Activation Capacity, Is Sufficient for Effective Trilineage Differentiation of ESCs. *Cell*

Reports, *20*(10), 2424–2438. https://doi.org/10.1016/j.celrep.2017.08.043

Nam, J. S., Turcotte, T. J., & Yoon, J. K. (2007). Dynamic expression of R-spondin family genes in mouse development. *Gene Expression Patterns*, *7*(3), 306–312. https://doi.org/10.1016/j.modgep.2006.08.006

Nichols, J., & Smith, A. (2009). Naive and Primed Pluripotent States. *Cell Stem Cell*, *4*(6), 487–492. https://doi.org/10.1016/j.stem.2009.05.015

Niehrs, C. (2010). On growth and form : a Cartesian coordinate system of Wnt and BMP signaling specifies bilaterian body axes. *Development*, *857*, 845–857. https://doi.org/10.1242/dev.039651

Oshima, H., Rochat, A., Kedzia, C., Kobayashi, K., & Barrandon, Y. (2001). Morphogenesis and renewal of hair follicles from adult multipotent stem cells. *Cell*, *104*(2), 233–245. https://doi.org/10.1016/S0092-8674(01)00208-2

Pittenger, M. F., Mackay, A. M., Beck, S. C., Jaiswal, R. K., Douglas, R., Mosca, J. D., … Marshak, D. R. (1999). Multilineage Potential of Adult Human Mesenchymal Stem Cells. *Science*, *284*(April), 143–148.

Qi, X., Li, T.-G., Hao, J., Hu, J., Wang, J., Simmons, H., … Zhao, G.-Q. (2004). BMP4 supports self-renewal of embryonic stem cells by inhibiting mitogen-activated protein kinase pathways. *Proceedings of the National Academy of Sciences*, *101*(16), 6027–6032. https://doi.org/10.1073/pnas.0401367101

Rao, T. P., & Kühl, M. (2010). An updated overview on wnt signaling pathways: A prelude for more. *Circulation Research*, *106*(12), 1798–1806.

https://doi.org/10.1161/CIRCRESAHA.110.219840

Recker, R. R., Benson, C. T., Matsumoto, T., Bolognese, M. A., Robins, D. A., Alam, J., … Myers, S. L. (2015). A randomized, double-blind phase 2 clinical trial of blosozumab, a sclerostin antibody, in postmenopausal women with low bone mineral density. *Journal of Bone and Mineral Research*, *30*(2), 216–224. https://doi.org/10.1002/jbmr.2351

Renard, C. A., Labalette, C., Armengol, C., Cougot, D., Wei, Y., Cairo, S., … Buendia, M. A. (2007). Tbx3 is a downstream target of the Wnt/β-catenin pathway and a critical mediator of β-catenin survival functions in liver cancer. *Cancer Research*, *67*(3), 901–910. https://doi.org/10.1158/0008-5472.CAN-06-2344

Ro, H., & Dawid, I. B. (2011). Modulation of Tcf3 repressor complex composition regulates cdx4 expression in zebrafish. *EMBO Journal*, *30*(14), 2894–2907. https://doi.org/10.1038/emboj.2011.184

Sáez, M. A., Fernández-Rodríguez, J., Moutinho, C., Sanchez-Mut, J. V., Gomez, A., Vidal, E., … Esteller, M. (2016). Mutations in JMJD1C are involved in Rett syndrome and intellectual disability. *Genetics in Medicine*, *18*(4), 378–385. https://doi.org/10.1038/gim.2015.100

Sathananthan, H., Pera, M., & Trounson, A. (2002). The fine structure of human embryonic stem cells. *Reproductive Biomedicine Online*, *4*(1), 56–61. https://doi.org/10.1016/S1472-6483(10)61916-5

Sierra, R. A., Hoverter, N. P., Ramirez, R. N., Vuong, L. M., Mortazavi, A., Merrill, B. J., … Donovan, P. J. (2018). *TCF7L1* suppresses primitive streak gene expression to

support human embryonic stem cell pluripotency. *Development*, dev.161075. https://doi.org/10.1242/dev.161075

Smith, A. G. (2001). Embryo-Derived Stem Cells: Of Mice and Men. *Cell*, *17*, 435–462. https://doi.org/10.1146/annurev.cellbio.17.1.435

Takahashi, S., Kobayashi, S., & Hiratani, I. (2018). Epigenetic differences between naïve and primed pluripotent stem cells. *Cellular and Molecular Life Sciences*, *75*(7), 1191–1203. https://doi.org/10.1007/s00018-017-2703-x

Tamai, K., Zeng, X., Liu, C., Zhang, X., Harada, Y., Chang, Z., & He, X. (2004). A Mechanism for Wnt Coreceptor Activation, *13*, 149–156. https://doi.org/10.1016/S1097-2765(03)00484-2

Thomson, J. a., Itskovitz-Eldor, J. (1998). Embryonic Stem Cell Lines Derived from Human Blastocysts. *Science*, *282*(5391), 1145–1147. https://doi.org/10.1126/science.282.5391.1145

Tumbar, T., Guasch, G., Greco, V., Blanpain, C., Lowry, W. E., Rendl, M., & Fuchs, E. (2004). Defining the Epithelial Stem Cell. *Science*, *303*(January), 359–363. https://doi.org/10.1126/science.1092436

Vacik, T., & Lemke, G. (2011). Dominant-negative isoforms of Tcf/Lef proteins in development and disease. *Cell Cycle*, *10*(24), 4199–4200. https://doi.org/10.4161/cc.10.24.18465

van Tienen, L. M., Mieszczanek, J., Fiedler, M., Rutherford, T. J., & Bienz, M. (2017). Constitutive scaffolding of multiple Wnt enhanceosome components by

legless/BCL9. *ELife*, *6*, 1–23. https://doi.org/10.7554/eLife.20882

Vldl, T., Arrow, P., Tamai, K., Semenov, M., Kato, Y., Spokony, R., … He, X. (2000). LDL-receptor-related proteins in Wnt signal transduction. *Nature*, *407*(6803), 530–535. https://doi.org/10.1038/35035117

Wang, R. N., Green, J., Wang, Z., Deng, Y., Qiao, M., Peabody, M., … Shi, L. L. (2014). Bone Morphogenetic Protein (BMP) signaling in development and human diseases. *Genes and Diseases*, *1*(1), 87–105. https://doi.org/10.1016/j.gendis.2014.07.005

Wiechens, N., & Fagotto, F. (2001). CRM1- and Ran-independent nuclear export of □ -catenin Nicola Wiechens and Franc ¸ ois Fagotto. *Current Biology*, *11*, 18–28.

Wilson, P. A., & Hemmati-brivanlou, A. (1995). Induction of Epidermis and Inhibitotion of Neural Fate by BMP4. *Nature*, (10), 331–333.

Winston, J. T., Strack, P., Beer-Romero, P., Chu, C. Y., Elledge, S. J., & Harper, J. W. (2008). The SCFbeta -TRCP-ubiquitin ligase complex associates specifically with phosphorylated destruction motifs in Ikappa Balpha and beta -catenin and stimulates Ikappa Balpha ubiquitination in vitro. *Genes & Development*, *13*(3), 270–283. https://doi.org/10.1101/gad.13.3.270

Wolf, D. H., & Hilt, W. (2004). The proteasome: A proteolytic nanomachine of cell regulation and waste disposal. *Biochimica et Biophysica Acta - Molecular Cell Research*, *1695*(1–3), 19–31. https://doi.org/10.1016/j.bbamcr.2004.10.007

Wu, C.-I., Hoffman, J. A., Shy, B. R., Ford, E. M., Fuchs, E., Nguyen, H., & Merrill, B. J. (2012). Function of Wnt/ -catenin in counteracting Tcf3 repression through the

Tcf3- -catenin interaction. *Development*, *139*(12), 2118–2129. https://doi.org/10.1242/dev.076067

Yang, J. (2018). SALL4 as a transcriptional and epigenetic regulator in normal and leukemic hematopoiesis, 1–9. https://doi.org/10.1186/s40364-017-0115-6

Yi, F., Pereira, L., Hoffman, J. A., Shy, B. R., Yuen, C. M., Liu, R., & Merrill, B. J. (2012). Opposing Effects of Tcf3 and Tcf1 Control Wnt-Stimulation of Embryonic Stem Cell Self Renewal. *Nat Cell Biology*, *13*(7), 762–770. https://doi.org/10.1038/ncb2283.Opposing

Ying, Q., Nichols, J., Chambers, I., & Smith, A. (2003). Cell 2003 Ying, *115*, 1–12. Retrieved from papers2://publication/uuid/0A219FD8-0097-41A6-9B78-A591BF1AF71F

Ying, Q., Wray, J., Nichols, J., Doble, B., Wray, J., Nichols, J., … Smith, A. (2008). The ground state of embryonic stem cell self-renewal. *Nature*, *453*(7194), 519–524. https://doi.org/10.1038/nature06968

Yue, X., Xiao, L., Yang, Y., Liu, W., Zhang, K., Shi, G., … Zhang, Q. (2015). High cytoplasmic expression of SALL4 predicts a malignant phenotype and poor prognosis of breast invasive ductal carcinoma. *Neoplasma*, *4*, 980–987. https://doi.org/10.4149/neo

Zeng, X., Tamai, K., Doble, B., Li, S., Huang, H., Habas, R., … He, X. (2005). A dual-kinase mechanism for Wnt co-receptor phosphorylation and activation. *Nature*, *438*(7069), 873–877. https://doi.org/10.1038/nature04185

Zhang, R., Geoffroy, V., Ridall, A. L., Karsenty, G., Tracy, T., Bonner, A. S., … Bonewald, L. F. (2000). Bone Resorption by Osteoclasts, *289*(September), 1504–1509.